J. Mech. Phys. Solids 178 (2023) 105344

Contents lists available at ScienceDirect

Journal of the Mechanics and Physics of Solids

journal homepage: www.elsevier.com/locate/jmps

On the structure of poroplastic constitutive relations

A. Amine Benzerga

Department of Aerospace Engineering, Texas A&M University, College Station, TX 77843, United States of America

ARTICLE INFO

Keywords:
Plasticity
Shear localization
Homogenization
Ductile fracture
Void growth
Mohr–Coulomb
Lode angle

ABSTRACT

The paper discusses from first principles all aspects relevant to the plasticity of porous materials. Emphasis is laid on unhomogeneous yielding, defined as the process of yielding and plastic flow under gradient-free macroscopically nonuniform deformation. The nonuniformity is represented by strain localization in one or more bands of finite thickness. A universal feature of all intrinsic yield criteria is their dependence upon the normal and shear tractions resolved on the band. When specialized to isotropy, a Mohr–Coulomb criterion and a Rankine–Tresca criterion emerge as two extremes. The latter is an ideal that typifies the yield behavior of porous materials under arbitrary loadings. The general theory stands for a finite number of bands or yield systems. Its overall structure bears some features of crystal plasticity, but with dependence upon the resolved normal stress. The evolution of microstructural parameters can be given in general terms, being solely based on the kinematic constraints of unhomogeneous yielding and matrix incompressibility. Throughout the paper, the competition with homogeneous yielding, heretofore taken for granted, is analyzed with or without strain and strain-rate hardening effects. We close by discussing the thermodynamic consistency of this new class of constitutive relations and a link to strain-gradient theories.

1. Introduction

Consider an incompressible, pressure-insensitive and ideally plastic matrix embedding some porosity. Then the effective behavior is compressible, pressure-dependent and not ideal-plastic. If normality of plastic flow is assumed for the matrix then it stands for the effective behavior under well-known conditions (Hill, 1950). There is a wealth of emergent complexity even for a simple matrix that obeys J_2 flow theory. To the neglect of pore shape evolution (and other sources of induced anisotropy), the yield criterion is J_2 and I_1 dependent (Green, 1972; Gurson, 1977). Any J_3 dependence that may have been shown later (Benallal et al., 2014; Leblond and Morin, 2014) is not significant enough to enlighten our understanding of experimental observations. In addition, porosity evolution follows from the yield criterion and the flow rule. This is attractive; but in practice, only the yield locus is governed by a variational principle, not the normal to it. For this reason, porosity evolution equations are heuristically enhanced (Tvergaard, 1982). This is particularly true when pore shape evolution is incorporated (Madou et al., 2013). Furthermore, softening is a natural outcome to porosity evolution. Hardening, on the other hand, has two components: matrix strain-hardening (often accounted for heuristically) and porosity evolution under circumstances where the porosity decreases (densification).

The above features of porous material plasticity endow its constitutive relations with a given structure. Some are universal but others are not. In any case, to date, the essential structure of poroplastic constitutive relations has been examined under macroscopically homogeneous deformation, either explicitly, through scale transition operations (Gurson, 1977; Ponte Castaneda and Suquet, 1997), or tacitly, e.g. Rousselier (1987). This leads to a class of constitutive relations for what we shall refer to as *homogeneous yielding*. There lies the main departure of the present work.

E-mail address: benzerga@tamu.edu.

https://doi.org/10.1016/j.jmps.2023.105344
Received 17 February 2023; Received in revised form 8 May 2023; Accepted 1 June 2023
Available online 7 June 2023

Here, we define a generic type of boundary conditions that allow for strain localization *within* the elementary volume. This leads to a class of constitutive relations for what we shall refer to as *unhomogeneous yielding*.[1] This type of behavior is relevant to *all* porous materials that may deform plastically: cellular, architected, materials with residual processing porosity, materials with deformation-induced porosity (ductile failure), nanoporous materials, as well as granular materials, save for internal friction effects that are not explicitly accounted for.

With these new boundary conditions as sole basis, along with results of classical (spatial) averaging and (where needed) new (ensemble-type) averaging, we uncover step by step the overall structure of poroplastic constitutive relations under unhomogeneous yielding. Many differences, as will be seen, emerge from the overall traits of homogeneous yielding. The competition between the two modes of yielding is discussed throughout.

In doing so, we have attempted not to leave out any aspect that is potentially of interest. Aspects that are addressed include: the general format of dissipation and yield functions; general features of isotropic yield surfaces; a general formulation for anisotropic constitutive relations including the evolution of microstructure; a differential hardening formulation; extensions to viscoplasticity and related issues; thermodynamic consistency; and a link to strain-gradient theory.

Throughout the paper, the aim is to discuss general features *a priori*, that is with no recourse to detailed calculations. By that we mean the type of calculations involved in operating scale transitions whether by means of analytical or computational modeling. Yet, no room is left for speculation.

The paper is organized following the order of the key elements listed above. Once the reader is familiar with the concept of unhomogeneous yielding developed in Section 2, the remaining sections may be, to some extent, read independently. There is a natural flow to the results that are obtained. For example, the extension to hardening in Section 7 cannot be fully appreciated without the fundamental result of Section 5.4.

Given the scope and length of the paper, many details are left out and key ones are reported in nine appendices. Some of these, e.g. Appendix A, contain known results but with original proofs. Other appendices contain completely new results, e.g. Appendices B and F.

2. Concept of unhomogeneous yielding

2.1. Macro-unhomogeneity

Consider a sample of material, the mechanical response of which is identified with the material's behavior. In a sample with heterogeneities, the exact boundary conditions on the sample's surface are generally not known. The boundary velocity must, however, satisfy the following relation:

$$D_{ij} \equiv \langle d_{ij} \rangle = \frac{1}{2V} \int_{\partial V} (v_i n_j + n_i v_j)\, \mathrm{d}S \tag{1}$$

where $\mathbf{D}$ and $\mathbf{d}(\mathbf{x})$ are respectively the overall and pointwise rates of deformation, $\mathbf{x}$ denoting the current position, V is the domain occupied by the sample, identified with its volume, $\mathbf{v}$ is the velocity and $\boldsymbol{n}$ the outward surface normal. The notation $\langle\cdot\rangle$ stands for spatial averaging over V.

Let $\boldsymbol{\Sigma} \equiv \langle \boldsymbol{\sigma} \rangle$ be the overall stress, $\boldsymbol{\sigma}(\mathbf{x})$ denoting the microscopic (Cauchy) stress. For any pair $\mathbf{d}$, $\boldsymbol{\sigma}$, not necessarily related constitutively, such that $\mathbf{d}$ is derivable from a continuous and kinematically admissible velocity $\mathbf{v}$, and $\boldsymbol{\sigma}$ is statically admissible, the following relation holds (see proof in Appendix A):

$$\langle \sigma_{ij}\, d_{ij} \rangle - \Sigma_{ij}\, D_{ij} = \frac{1}{V} \int_{\partial V} \big(\sigma_{ij} - \langle \sigma_{ij} \rangle\big) n_j \big(v_i - \langle v_{i,k} \rangle x_k\big)\, \mathrm{d}S \tag{2}$$

Of particular interest are boundary conditions that would make the right-hand side of Eq. (2) vanish, i.e. satisfy the following equality:

$$\langle \sigma_{ij}\, d_{ij} \rangle = \Sigma_{ij}\, D_{ij} \tag{3}$$

When applicable, the above statement embodies the Hill–Mandel lemma (Hill, 1967; Mandel, 1964). A sufficient condition for Eq. (3) to hold is that the boundary velocity be given by[2]:

$$\forall\, \mathbf{x} \in \partial V, \qquad v_i = D_{ij} x_j \tag{4}$$

Eq. (4) defines *macroscopically homogeneous* deformation, or *uniform constraint* in the sense of Hill (1967).

For more general, say periodic boundary conditions of the form:

$$\forall\, \mathbf{x} \in V, \qquad v_i = (D_{ij} + \Omega_{ij}) x_j + \tilde{v}_i \tag{5}$$

[1] The reader familiar with the physics of plasticity may argue that plastic deformation is always non-homogeneous at some scale. The best way to escape triviality is to invent a new word that is consistent with the rules of the language!

[2] Uniform loading in the sense of Hill would also satisfy Eq. (3), as is well known.

where Ω_{ij} denotes the spin and $\tilde{v}_i$ a periodic field, one readily obtains from Eq. (2) and the zero-mean property of fluctuations:

$$\langle \sigma_{ij}\, d_{ij} \rangle - \Sigma_{ij}\, D_{ij} = \frac{1}{V} \int_{\partial V} t_i \tilde{v}_i \, \mathrm{d}S \tag{6}$$

with $t_i = \sigma_{ij} v_j$ the traction. Thus, if the sample is a cube of side l, supposed to be under uniform constraint, and if Eq. (5) is viewed as applicable over a period $\bar{x}$, then the right hand-side of Eq. (6) is of order $\bar{x}/l$. Typically, $\bar{x}$ is the mean spacing between heterogeneities. By way of consequence, Eq. (3) can be satisfied as we please provided that $l/\bar{x}$ is sufficiently large. This provides a basis for so-called macroscopically homogeneous systems and macroscopically uniform loading or constraint (Hill, 1967).

The above definitions are, however, not sufficiently precise for our purposes, i.e. for a range of plasticity-mediated localization and failure phenomena. Consider a macroscopic specimen subjected to whatever boundary conditions may be applied to it in a physical experiment. These are generally of mixed character. Boundary conditions prevailing at critical locations are generally not known. Therefore, in developing a constitutive law applicable at such locations boundary conditions must be general enough to allow for a range of emergent behaviors, yet simple enough to calculate a constitutive response. To fix ideas, we foresee that deformation may concentrate in one or more bands, the orientation of which is set by the dense packing of heterogeneities, Fig. 1. Band thickness is limited by the mean heterogeneity size.

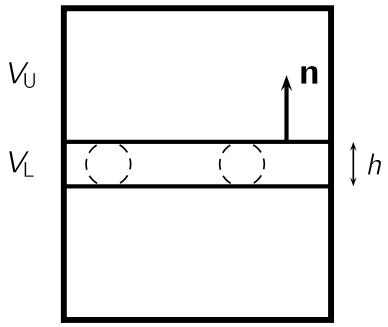

Fig. 1. Material element with a band of finite strain concentration.

Boundary conditions that accommodate strain concentration in a band are of the type:

$$\forall\, \mathbf{x} \in \partial V_L, \qquad \mathbf{v} = (\mathbf{L} + \bar{\boldsymbol{\Omega}})\mathbf{x} \tag{7}$$

$$\forall\, \mathbf{x} \in \partial V_U, \qquad \mathbf{v} = \mathbf{U}\mathbf{x} + \mathbf{v}_0 \tag{8}$$

where $\mathbf{L}$ and $\mathbf{U}$ are constant second-rank symmetric tensors, $\bar{\boldsymbol{\Omega}}$ is constant and skew-symmetric, and $\mathbf{v}_0$ is a constant velocity introduced to ensure interfacial continuity. That the $\mathbf{v}_0$ of Eq. (8) is constant is made possible thanks to a judicious choice of $\bar{\boldsymbol{\Omega}}$ in Eq. (7). Also, ∂V_L and ∂V_U respectively denote the boundaries of domains V_L and V_U occupied by the band and region outside of it. If potential dilation is confined to the band then $\mathbf{U}$ is traceless. Let $\mathbf{n}$ denote the outward normal to the band, h its thickness and $c \equiv V_L/V$ its volume fraction. The difference in strain rate between the two regions takes the form (see Appendix B for a proof):

$$\mathbf{L} - \mathbf{U} = \frac{1}{h} \mathbf{v}_0 \otimes^{\mathrm{s}} \mathbf{n} \tag{9}$$

where $\mathbf{v}_0/h$ is related to the overall rate of deformation by:

$$\frac{c}{h} \mathbf{v}_0 = \frac{1}{2} D_{kk} \mathbf{n} + D_{nm} \mathbf{m} \tag{10}$$

Here, $\mathbf{m}$ is a unit vector parallel to the band in the direction of resolved shear D_{nm}. Also, $\otimes^{\mathrm{s}}$ denotes the symmetric dyadic product. The general format of Eq. (9) simply follows from overall strain-rate compatibility. On the other hand, Eq. (10) is more specific to the present theory and follows from the definition of the overall rate of deformation $\mathbf{D}$, velocity continuity across the interface and a judicious choice of $\bar{\boldsymbol{\Omega}}$; see Appendix B for details.

The boundary conditions defined by Eqs. (7) and (8) with data given by Eqs. (9) and (10) satisfy the Hill–Mandel lemma, Eq. (3). That they do not correspond to uniform constraint is obvious. But they also make the right-hand side of Eq. (6) vanish for arbitrary $l/\bar{x}$. Assuming an appropriate shape of V, these boundary conditions are, to be sure, a subset of periodic boundary conditions, Eq. (5), with a piece-wise linear fluctuation. The vanishing of the right-hand side of Eq. (6) then results from traction equilibrium, written separately for the band and the entire volume.

Eqs. (7) to (10) define *macroscopically unhomogeneous* deformation. That they are relevant in discussing a range of unhomogeneous yield phenomena can only be made clear further below.

2.2. Limitation of localization theory

In the basic form of strain localization theory, as eventually settled in (Rice, 1976), a bifurcation is sought within a localized band of orientation $\mathbf{n}$ across which the jump in deformation gradient rate is necessarily given by:

$$\dot{\mathbf{F}} - \dot{\mathbf{F}}_0 = \mathbf{q} \otimes \mathbf{n} \tag{11}$$

where $\mathbf{F}$ is the deformation gradient, $\mathbf{F}_0$ its value for a homogeneous solution (or outside the band) and $\mathbf{q}$ is some vector-valued function of position across the band. Then using an incremental constitutive relation, which is tacitly assumed to hold uptil the critical point, the equations of continuing equilibrium lead to the governing equation for the kinematical non-uniformity $\mathbf{q}$ in Eq. (11). A necessary condition for the onset of localization is then:

$$\det(\mathbf{n}\,\mathbb{L}\,\mathbf{n}) = 0 \tag{12}$$

where $\mathbb{L}$ denotes the tensor of moduli entering the incremental relation between $\mathbf{F}$ and the nominal (first Piola-Kirchhoff) stress, $\mathbf{P}$.

In the theory of unhomogeneous yielding, boundary conditions (7)–(9) may be recast in the form: $\dot{\mathbf{x}} = \dot{\mathbf{F}}\mathbf{X}$ inside the band, $\dot{\mathbf{x}} = \dot{\mathbf{F}}_0\mathbf{X} + \dot{\mathbf{x}}_0$ outside the band with the necessary jump relation: $\dot{\mathbf{F}} - \dot{\mathbf{F}}_0 = \frac{1}{h}\dot{\mathbf{x}}_0 \otimes \mathbf{n}$, such that a parallel may be drawn with Eq. (11). In addition, the restated boundary conditions may be shown to satisfy an appropriate form of the Hill–Mandel lemma in terms of $\mathbf{F}$, $\mathbf{P}$ and their microscopic counterparts.

There is an obvious difference between the theory of strain localization, in its basic form recalled above, and the theory of unhomogeneous yielding in that a homogeneous solution is *not* a possible solution in the latter.

A closer parallel may indeed be drawn with an imperfection band analysis. As shown by Rice (1976), that analysis can be recast in the general framework of strain localization. The compatibility requirement of Eq. (11) remains valid with $\mathbf{q}$ now interpreted as the rate of (accumulated) deformation non-uniformity. The localization condition, Eq. (12), also remains valid and the relevance of the analysis essentially manifests in that the field inside the band can be driven to localization well before the moduli of the field outside the band would allow.

Still, there are some major differences between the imperfection band version of strain localization theory and the theory of unhomogeneous yielding. Chief among these is that one condition of applicability of strain localization theory is that the (macroscopic) constitutive law must remain valid up to the critical point. Now, constitutive laws are typically either posited (eventually guided by thermodynamic considerations) or derived while assuming macroscopically homogeneous deformation, as embodied in Eq. (4). Employing such a constitutive law up to the critical point implies accepting the validity of boundary conditions (4) up to the critical point. This is not taken for granted in the theory of unhomogeneous yielding.

In fact, so far we have merely been concerned with kinematical considerations underlying the concept of macroscopically unhomogeneous deformation. No constitutive description has yet been put forth. We have only raised the possibility that more general boundary conditions could give rise to a better constitutive description, using a metric that is yet to be elucidated.

Furthermore, by construction the band in strain localization theory undergoes infinite strain concentration and may be of vanishingly small thickness. By way of contrast, we are after a theory of *finite* strain concentration in one or more bands of *finite* thickness. In a sense, the theory aims at "homogenizing" a material containing such bands.

2.3. Limitation of homogenization theory

The ground for possibility of any homogenization in material modeling demands separation of scales. The theory of unhomogeneous yielding to be developed herein is no exception. It is important that the scope and limits of the theory be so defined. What is of particular importance, however, is that unhomogeneous yielding may set in well before any separation of scales breaks down.

While it is generally desirable that a constitutive theory emerges from some homogenization framework, the organic dependence of any homogenization upon boundary conditions is problematic when different choices of these deliver vastly disparate responses. Also, homogenization theory fails to account for the change in boundary conditions themselves in an evolution problem.

In porous material plasticity, all constitutive relations have common traits so long as unhomogeneous yielding prevails. We shall analyze these, keeping two things in mind:

1. When separation of scales holds, the constitutive relation is valid within rigorous bounds of homogenization theory.
2. When it does not, the theory of unhomogeneous yielding is still the most appropriate one to employ at critical locations.

3. Dissipation function

The implications of the choice of boundary conditions in developing a constitutive theory are presented here for rate-independent materials. A useful framework for discussing the structure of constitutive laws is that of limit analysis. We briefly recall its principle and discuss emergent behavior that can be anticipated when macroscopically unhomogeneous deformation is considered. Similar conclusions are attained using the notion of effective potentials in nonlinear homogenization (Ponte Castaneda and Suquet, 1997).

3.1. Limit load theory

Classical limit analysis typically applies to elastic–ideal plastic materials under small transformations, and to rigid-ideal plastic materials under finite deformation. In what follows, the latter situation is assumed; see Leblond et al. (2018) for an appraisal of earlier works (Hill, 1951; Drucker et al., 1952) and conditional extensions to elasticity, finite deformation and strain-hardening.[3] For a plastically incompressible matrix, obeying some associated yield criterion, the plastic dissipation[4] is given by:

$$\pi(\mathbf{d}) = \sup_{\boldsymbol{\sigma}^* \in \mathcal{C}} \sigma^*_{ij}\, d_{ij} \tag{13}$$

where C is the convex of reversibility and $\mathbf{d}$ is traceless. Let $\mathbf{v}(\mathbf{x})$ be a kinematically admissible velocity field, that is, obeying either macro-homogeneity, Eq. (4), macro-unhomogeneity, Eqs. (7) and (8), or more generally Eq. (5) with sufficiently large $l/\bar{x}$. Let $\boldsymbol{\sigma}$ be a statically and plastically admissible stress field. Then, from Eqs. (3) and (13)

$$\forall \mathbf{d}, \quad \boldsymbol{\Sigma} : \mathbf{D} \leq \langle \pi(\mathbf{d}) \rangle \tag{14}$$

If the heterogeneities are voids, appropriate extensions of stress and velocity fields in the voids are assumed (Benzerga and Leblond, 2010). A tighter bound is obtained by introducing the overall dissipation Π associated with $\mathbf{D}$:

$$\forall \mathbf{D}, \quad \boldsymbol{\Sigma} : \mathbf{D} \leq \Pi(\mathbf{D}) \equiv \inf_{\mathbf{v} \in \mathcal{K}(\mathbf{D})} \langle \pi(\mathbf{d}) \rangle \tag{15}$$

where $\mathcal{K}(\mathbf{D})$ denotes the set of kinematically admissible velocity fields consistent with $\mathbf{D}$. The macroscopic domain of reversibility is defined as:

$$\mathscr{C} = \{ \boldsymbol{\Sigma} \mid \forall \mathbf{D},\ \boldsymbol{\Sigma} : \mathbf{D} \leq \Pi(\mathbf{D}) \} \tag{16}$$

the boundary of which is the yield surface. Regular portions of the latter are parametrically defined by:

$$\Sigma_{ij} = \frac{\partial \Pi}{\partial D_{ij}}(\mathbf{D}) \tag{17}$$

See e.g. Benzerga and Leblond (2010) for details and further references.

3.2. Anticipated features

It appears immediately from Eq. (15) that the value of $\Pi(\mathbf{D})$ depends on the type of boundary conditions used. Given a prescribed macroscopic rate of deformation, let Π^{H}, Π^{P}, Π^{U} respectively denote the values obtained with infima in Eq. (15) sought in the sets $\mathcal{K}^{\mathrm{H}}$, $\mathcal{K}^{\mathrm{P}}$, $\mathcal{K}^{\mathrm{U}}$, which correspond to boundary conditions (4), (5) and (7)–(10), respectively. Since $\mathcal{K}^{\mathrm{P}} \supset \mathcal{K}^{\mathrm{H}}$ and $\mathcal{K}^{\mathrm{P}} \supset \mathcal{K}^{\mathrm{U}}$ we always have $\Pi^{\mathrm{P}} \leq \Pi^{\mathrm{H}}$ and $\Pi^{\mathrm{P}} \leq \Pi^{\mathrm{U}}$. This means that periodic boundary conditions are preferable for obtaining a tighter upper bound and a better approximation of the exact velocity field. However, the two sets $\mathcal{K}^{\mathrm{H}}$ and $\mathcal{K}^{\mathrm{U}}$ are entirely different so that, in general, one does not know how Π^{H} and Π^{U} are rank-ordered.

In general, therefore, there is competition between homogeneous and unhomogeneous yielding. Whether one or the other prevails can only be determined if both Π^{H} and Π^{U} are evaluated. Additional uncertainty arises in practical evaluations, as one does not exhaustively explore the sets $\mathcal{K}^{\mathrm{H}}$ and $\mathcal{K}^{\mathrm{U}}$. Thus, dissipation values under periodic boundary conditions, Π^{P}, constitute a benchmark against which analytical estimates ought to be compared. Typically, such benchmarks are determined numerically.

Alternatively, assume now boundary conditions given by (7)–(9) with $\mathbf{v}_0$ being either $\mathbf{0}$ or given by (10). The former case reduces to uniform constraint. If $\mathcal{K}^{\mathrm{U}}$ is reinterpreted this way then clearly $\mathcal{K}^{\mathrm{U}} \supset \mathcal{K}^{\mathrm{H}}$ and, by way of consequence we always have: $\Pi^{\mathrm{P}} \leq \Pi^{\mathrm{U}} \leq \Pi^{\mathrm{H}}$. Thus, boundary conditions (7)–(9) lead to a constitutive model that unifies homogeneous and unhomogeneous yielding.

For porous materials, the class of homogeneous yield models includes Gurson's (1977) and like models. On the other hand, unhomogeneous yield models with closed-form expressions of Π^{U} are relatively recent (Benzerga and Leblond, 2014). An example of a unified model, i.e. that combines homogeneous and unhomogeneous yielding, was developed by Morin et al. (2016).

An important question is whether there is ground to expect unhomogeneous versus homogeneous yielding to prevail for certain types of loading. In porous material plasticity, some quantitative answers are available in the literature for specific geometries. One finds that homogeneous yielding is favored in simple tension and low stress triaxiality tension, but only conditionally, namely for near-axisymmetric states. On the other hand, unhomogeneous yielding always prevails for shear states, irrespective of superposed hydrostatic stress, and for high-triaxiality tensile states, irrespective of superposed shear. It is as important to point out that these trends hold in the absence of strain hardening or with hardening incorporated heuristically as proposed by Gurson (1977). This follows from the absence of hardening in classical limit load theory recalled in Section 3.1. Rationales, if only qualitative, are given below for the above stated trends. Quantitative proofs are forthcoming.

[3] In particular, the theory is rigorous for limit states, but does not account for elastic–plastic couplings that occur below such states, as would arise in cavitation instabilities (Huang et al., 1991) or ultra-low cycle void-mediated fatigue (Morin et al., 2017).

[4] This denomination is adequate in view of what follows. As defined, $\pi(\mathbf{d})$ simply stands as the support function of C, $\mathbf{d}$ being any symmetric second-order tensor.

3.2.1. Simple tension

In accordance with Eq. (10), unhomogeneous yielding in the absence of shear corresponds to a state of uniaxial deformation normal to the band ($D_{\alpha\alpha} = 0$, no sum on $\alpha \neq n$). Without porosity this state would be impossible in an incompressible material. Not only does its possibility require porosity but also sufficient dilation. But the latter is minimal to inexistent in simple tension, unless the porosity is sufficiently large. Thus, unhomogeneous yielding is unlikely in simple tension.

3.2.2. Simple shear

By way of contrast, Eq. (10) implies that unhomogeneous deformation is possible in shear by simply concentrating the shear within the band with no constraint on dilational flow. In shear, therefore, the competition between unhomogeneous and homogeneous yielding hinges on which mode of deformation dissipates less, in the sense of the governing variational principle. For certain pore arrangements, this question was actually addressed by Drucker (1966) with unhomogeneous yielding unequivocally providing the lowest dissipation. The question of how strain hardening affects this competition remains unsettled (see Section 7 for more details.)

3.2.3. Tension states

Consider the case of simple tension as reference and increasingly superpose a hydrostatic pressure p (positive for tension). For sufficiently low values of p, the driving force for dilation remains too small to accommodate a state of uniaxial deformation perpendicular to some potential band, i.e. to a state of unhomogeneous yielding in tension, unless the porosity is sufficiently large. There is a minimum value of p above which that state becomes possible and, in fact, favored. This minimum must be porosity dependent.

3.2.4. Shear states

Consider the case of simple shear as reference and increasingly superpose a hydrostatic pressure p. For vanishingly small porosity, the limit load would be independent of the value of p. Yet, the dissipation with the strain rate concentrated in a band would be lower than with it diffuse. It is plausible therefore that for any value of p, superposed onto a state of shear, unhomogeneous yielding would remain the favorable mode, particularly in the absence of hardening.

3.3. Reduced form

For unhomogeneous yielding, there is no extensional strain-rate parallel to the band. Therefore, the overall dissipation function Π only depends on the strain rate normal to the band and the shear strain rate resolved onto the band. We exploit these strong kinematic constraints to write a reduced dissipation function in the form $\Pi(\dot{\epsilon}, \dot{\gamma})$, keeping the notation Π and using the identities $\dot{\epsilon} \equiv D_{nn}$ (no sum on n) and $\dot{\gamma} \equiv D_{nm}$.

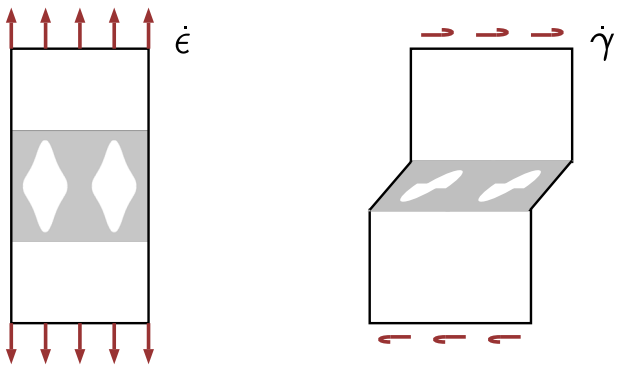

Fig. 2. The two modes of unhomogeneous yielding. (a) Opening. (b) Sliding.

Fig. 2 depicts the two fundamental modes of unhomogeneous yielding. In the opening mode, Fig. 2a, the deformation is uniaxial with $\dot{\epsilon}$ as the sole kinematic descriptor. In the sliding mode, Fig. 2b, $\dot{\gamma}$ is the only kinematic descriptor. In general, deformation consists of a combination of these two modes during unhomogeneous yielding. Both opening and sliding are pore-mediated. For opening, mediation is through internal necking (i.e. formation of a neck in the inter-pore ligament). For sliding, mediation is through void shearing.

4. Yield criterion

4.1. Principle of derivation

An effective yield criterion in the form $\phi(\boldsymbol{\Sigma}) = 0$ may be obtained by eliminating $\mathbf{D}$ from either the parametric form of the yield locus, Eq. (17), or the fundamental inequality of limit analysis, Eq. (15). Both sides of the inequality are homogeneous of degree 1 in $\mathbf{D}$. In particular, elimination of $\mathbf{D}$ from Eq. (17) is possible since $\partial \Pi / \partial \mathbf{D}$ is positively homogeneous of degree 0.

4.2. Anticipated features

Hill's principle of maximum plastic work applies overall if it is assumed to hold in the matrix and elastic strains are neglected (the Hill–Mandel lemma is a useful instrument to prove this.) The reversibility domain $\mathscr{C}$, Eq. (16), is therefore convex and the plastic rate of deformation belongs to the hypercone of normals to the effective yield surface. Furthermore, if the latter is smooth then the overall flow obeys normality.

By way of consequence, a reduced form of the yield criterion is possible for unhomogeneous yielding. Since the extensional strain-rate parallel to the band vanishes, normality of plastic flow implies that ϕ is independent of normal stresses parallel to the band. Unhomogeneous yielding is only dependent upon the stress normal to the band and possibly upon the shear stress resolved onto the band. These are denoted σ and τ, respectively. In general, therefore, any criterion of unhomogeneous yielding may be written in the reduced form: $\phi(\sigma, \tau) = 0$ using the above definitions.

4.3. Example yield criteria

Eqs. (15) and (17) provide a variational characterization of the effective yield surface. A specific yield criterion obtains by considering as given the matrix flow model (in particular defining the boundary of domain C entering Eq. (13)) and the geometry (shapes of external domain V and heterogeneity). In an upper-bound approach, a subset of $\mathcal{K}$ in Eq. (15) is also given. The procedure is generally tedious even when limited to relatively simple geometries.

Here, we are not interested in specific yield function derivations. Yet, in the spirit of discussing the overall structure of constitutive relations *a priori*, we shall illustrate the various forms of yield criteria that would emerge from certain admitted forms of the dissipation function, limiting our attention to unhomogeneous yielding, that is using the general properties of any subset of $\mathcal{K}^{\mathrm{U}}$ in Eq. (15).

As discussed in Section 3.3 the main outcome is that the dissipation function may be given in reduced form, which we will further simplify by dropping all dots, keeping in mind that the arguments are rates: $\Pi(\epsilon, \gamma)$.

Typical results are condensed in Table 1. The dissipation function must be positively homogeneous of degree one. With no claim of completeness, it may be written in dimensionless form as the sum of any number of functions having the form:

$$\Pi(\epsilon, \gamma) = \frac{\left(|\epsilon|^n + |\gamma|^n\right)^{\frac{1}{m}}}{\left(|\epsilon|^p + |\gamma|^p\right)^{\frac{1}{q}}}, \qquad \frac{n}{m} - \frac{p}{q} = 1 \tag{18}$$

with integers n, m, p, q satisfying the above constraint and any coefficients of the various terms omitted to lighten the writing.

Regular parts of the yield locus are defined by specializing Eq. (17) as:

$$\sigma = \frac{\partial \Pi}{\partial \epsilon} \qquad \text{and} \qquad \tau = \frac{\partial \Pi}{\partial \gamma} \tag{19}$$

Thus, using the property

$$\Pi(\epsilon, \gamma) = |\epsilon|\, \Pi(1, P) \qquad \text{with} \qquad P \equiv \frac{\gamma}{\epsilon} \tag{20}$$

one gets

$$\begin{cases} \sigma = \Pi \dfrac{\partial \ln \Pi}{\partial \epsilon} = \operatorname{sgn} \epsilon \; \Pi(1, P) \left[\operatorname{sgn} \epsilon - \dfrac{n}{m} \dfrac{|P|^n}{1 + |P|^n} + \dfrac{p}{q} \dfrac{|P|^p}{1 + |P|^p} \right] \\ \tau = \Pi \dfrac{\partial \ln \Pi}{\partial \gamma} = \operatorname{sgn} \gamma \; \Pi(1, P) \left[\dfrac{n}{m} \dfrac{|P|^{n-1}}{1 + |P|^n} - \dfrac{p}{q} \dfrac{|P|^{p-1}}{1 + |P|^p} \right] \end{cases} \tag{21}$$

which constitutes a parametric representation of the regular part of the yield locus, if a single function of the type of Eq. (18) is used.

Elimination of parameter P from Eq. (21) is possible in some cases, leading to a closed-form expression of the yield criterion. Take for instance $n = 2$, $m = 2$, $p = 0$, $q \neq 0$. The corresponding dissipation function is shown in the second row of Table 1. In this case, elimination of P from Eq. (21) leads to an elliptic criterion. If two functions are used, the first as above and the second corresponding to $n = 1$, $m = 1$, $p = 0$, $q \neq 0$ with the coefficient of, say, γ being nil, then the yield surface would exhibit regular parts and singular parts. The regular part would still be given by a quadratic function. This case is listed on the fourth row in Table 1. Both criteria are relevant to void coalescence under combined tension and shear; see Tekoglu et al. (2012) for an elliptic criterion and Torki et al. (2015) for the criterion labeled TBL in Table 1.

Table 1
Dissipation, intrinsic yield functions and surfaces for unhomogeneous yielding.

Dissipation, $\Pi(\epsilon,\gamma)$	Yield function, $\phi(\sigma,\tau)$	Yield surface	Type
$\lvert\epsilon\rvert + \lvert\gamma\rvert$	$\max\{\lvert\sigma\rvert, \lvert\tau\rvert\} - 1$	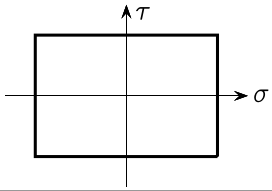	Rankine–Tresca
$\sqrt{\epsilon^2+\gamma^2}$	$\sigma^2 + \tau^2 - 1$	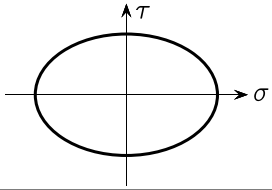	Elliptic
$\sqrt{\epsilon^2+\gamma^2} + \epsilon$	$(\sigma-1)^2 + \tau^2 - 1$	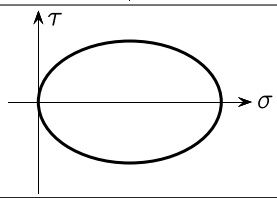	"Cam-Clay"
$\sqrt{\epsilon^2+\gamma^2} + \lvert\epsilon\rvert$	$(\lvert\sigma\rvert-1)^2 + \tau^2 - 1$ for $\lvert\sigma\rvert \geq 1$ $\lvert\tau\rvert - 1$ for $\lvert\sigma\rvert \leq 1$	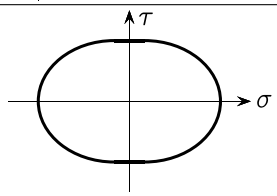	TBL
$\dfrac{\epsilon^2+\gamma^2}{\lvert\gamma\rvert}$	$\frac{1}{4}\sigma^2 + \lvert\tau\rvert - 1$	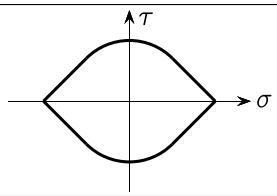	"Beams"

Interestingly, if the absolute value is omitted in the latter example, one obtains a Cam-Clay like surface. If the case $n = 1$, $m = 1$, $p = 0$, $q \neq 0$ is treated separately with both coefficients then a Rankine–Tresca[5] surface is obtained (first row in Table 1). The last reported case for $n = 2$, $m = 1$, $p = 1$, $q = 1$, with the coefficient of γ taken to be zero in the denominator, arises in some problems of structural mechanics, namely in the limit design of beams under combined bending and extension. If the coefficient of γ is not zero, then a similar yield surface is obtained, which is rotated by an angle that depends on the ratio of coefficients in the denominator.

Whenever the set of integers in Eq. (18) contains an odd number, absolute values would appear in the expression of the dissipation, which make the latter non-differentiable at some points. In such cases, the parametric representation of Eq. (21) holds only for regular parts (e.g. the TBL criterion) or not at all (e.g. the Rankine–Tresca criterion). To obtain the singular parts, a method summarized in Appendix C may be used. Incidentally, the entire yield surface of the last example may be obtained using the parametric representation, the only singular point in this case being the corner on the σ axis. The non-differentiability of Π at some points does not necessarily lead to corners on the yield locus. As seen in Table 1 the yield loci of the first and last examples exhibit corners while the TBL locus does not.

There are many more examples than given in Table 1 or embodied in representations such as that of Eq. (18). Nevertheless, the subfamily of dissipation functions having $n = m$, $p = 0$, $q \neq 0$ are of particular interest. The first two members $n = 1$ and $n = 2$ are the Rankine–Tresca and elliptic criteria listed in the first two rows of Table 1. All subsequent ones (for $n \geq 3$) have corners on both axes. The higher the value of n the sharper the corners. In the limit $n \to \infty$ a Mohr–Coulomb type yield criterion is obtained. The writer is not aware of derivations from first principles of a Mohr–Coulomb criterion.

[5] The reader familiar with plasticity theory would find this denomination appropriate, even though there is no such a thing as a Rankine–Tresca criterion in the literature.

5. Isotropic behavior

If plastic deformation is unhomogeneous at some scale of description then the dissipation potential, at that same scale, may only depend on resolved rates of deformation. The yield criterion may then only depend on resolved normal and shear stresses. The number of bands of strain concentration and their orientations depend on the spatial distribution of voids. If that distribution is statistically homogeneous then the effective behavior is isotropic and the effective yield criterion may be determined by probing all possible band orientations. In this section, we examine the generic form of the overall isotropic yield criterion that would emerge from considering various forms of intrinsic yield criteria at the individual band level as, for example, reported in Table 1.

5.1. General procedure

We revisit and generalize a procedure by Keralavarma (2017). Let $\phi(\sigma,\tau)=0$ be the yield criterion[6] associated with a system of unhomogeneous yielding defined by band orientation $\mathbf{n}$. The resolved normal stress, σ, and resolved shear stress, τ, are given by[7]:

$$\sigma = \mathbf{n}\cdot\boldsymbol{\sigma}\mathbf{n} \quad , \quad \tau^2 = \mathbf{n}\cdot\boldsymbol{\sigma}^2\mathbf{n} - (\mathbf{n}\cdot\boldsymbol{\sigma}\mathbf{n})^2 \tag{22}$$

A macroscopically isotropic yield surface is obtained as the envelope of yield surfaces $\phi(\sigma,\tau)=0$ indexed by $\mathbf{n}$ underlying the definitions in Eq. (22). An effective yield function may thus be obtained as:

$$\Phi(\boldsymbol{\sigma}) = \max_{\mathbf{n}\in\partial\mathcal{B}} \phi(\sigma,\tau) \tag{23}$$

where $\mathcal{B}$ denotes the unit ball, i.e. $\partial\mathcal{B}\equiv\{\mathbf{n}\,|\,\mathbf{n}\cdot\mathbf{n}=1\}$.

A necessary condition for the existence of an orientation $\mathbf{n}$ maximizing ϕ is (see Appendix D):

$$\left[\left(f(\sigma)-\frac{\sigma}{\tau}g(\tau)\right)\boldsymbol{\sigma}+\frac{1}{2\tau}g(\tau)\boldsymbol{\sigma}^2\right]\mathbf{n}=\lambda\mathbf{n} \tag{24}$$

where

$$f(\sigma)=\frac{\partial\phi}{\partial\sigma} \quad \text{and} \quad g(\tau)=\frac{\partial\phi}{\partial\tau} \tag{25}$$

Functions f and g may generally depend on both the normal and shear stresses, but most intrinsic criteria of interest have a structure consistent with the above relations. It is convenient for what follows to write the necessary condition as:

$$\left[F(\sigma,\tau)\boldsymbol{\sigma}+G(\tau)\boldsymbol{\sigma}^2\right]\mathbf{n}=\lambda\mathbf{n} \tag{26}$$

with F and G identified from Eq. (24). Two exclusive sets of (potential) solutions are conceivable. Either $\mathbf{n}$ lies in a principal plane of loading or it does not. A special case of the former is when $\mathbf{n}$ is along a principal direction of loading. It is evident from Eq. (26) that any eigenvector of $\boldsymbol{\sigma}$ is indeed a solution. We shall refer to that as *normal yielding*.

More generally, let $\mathbf{n}=n_i\mathbf{e}_i$ where $\mathbf{e}_i$ are the unit eigenvectors of $\boldsymbol{\sigma}$. Proceeding by strict equivalence, Eq. (26) becomes:

$$\begin{cases} \forall i, \quad F\sigma_i+G\sigma_i^2=\lambda & \{\text{I}\} \\ \text{OR} & \\ \exists i\,|\,n_i=0 \quad \text{AND} \quad \forall j\neq i, \quad F\sigma_j+G\sigma_j^2=\lambda & \{\text{II}\} \end{cases} \tag{27}$$

where σ_i denotes a principal stress.

With no loss of generality, family {I} of potential solutions must satisfy:

$$\begin{cases} F+G(\sigma_1+\sigma_2)=0 \quad \text{AND} \quad F+G(\sigma_2+\sigma_3)=0 \quad \text{AND} \quad \sigma_1\neq\sigma_2\neq\sigma_3 \\ \text{OR} \\ F+G(\sigma_1+\sigma_2)=0 \quad \text{AND} \quad \sigma_1\neq\sigma_2 \quad \text{AND} \quad \sigma_3=\sigma_1 \end{cases} \tag{28}$$

where the principal stresses are considered in no particular order. The first subfamily in Eq. (28) is the empty set. Indeed, the first two conditions in Eq. $(28)_1$ imply $\sigma_1=\sigma_3$, and this contradicts the last condition. Thus, the only possible solutions from family {I} must satisfy Eq. $(28)_2$. In this case, one principal stress has multiplicity of (at most) 2, which implies that any vector in the $\mathbf{e}_1$–$\mathbf{e}_3$ plane is an eigenvector. With no loss of generality, therefore, one may take $n_3=0$, such that yielding occurs by combined tension and shear in the $\mathbf{e}_1$–$\mathbf{e}_2$ plane.

Next, family {II} of potential solutions must satisfy:

$$\begin{cases} n_3=0 \quad \text{AND} \quad F(\sigma_1-\sigma_2)+G(\sigma_1^2-\sigma_2^2)=0 & \{\text{IIa}\} \\ \text{OR} & \\ n_2=n_3=0 \quad \text{AND} \quad F\sigma_1+G\sigma_1^2=\lambda & \{\text{IIb}\} \end{cases} \tag{29}$$

[6] The criterion $\phi(\sigma,\tau)=0$ could have been arrived at by taking any isotropic yield criterion in the pore-free matrix. However, to avoid unnecessary complications and appreciate the significance of the results that follow, the reader may assume that plastic flow in the matrix obeys J_2 theory.

[7] In this and subsequent sections, we use $\boldsymbol{\sigma}$ for what was denoted $\boldsymbol{\Sigma}$ in previous sections, now that "homogenization" is out of context.

Subfamily {IIb} corresponds to $\mathbf{n}$ being along a principal stress direction. That eigenvectors of $\boldsymbol{\sigma}$ are possible solutions was evident from Eq. (26), as noted above. This subfamily of solutions corresponds to normal yielding. Now, {IIa} itself admits two possibilities:

$$\begin{cases} n_3 = 0 \quad \text{AND} \quad F + G(\sigma_1 + \sigma_2) = 0 \quad \text{AND} \quad \sigma_1 \neq \sigma_2 \quad \{\text{IIaa}\} \\ \text{OR} \\ n_3 = 0 \quad \text{AND} \quad \sigma_1 = \sigma_2 \quad \{\text{IIab}\} \end{cases} \tag{30}$$

In subfamily {IIab} one principal stress has multiplicity of (at least) 2, which implies that any vector in the $\mathbf{e}_1$–$\mathbf{e}_2$ plane is an eigenvector. With no loss of generality, therefore, one may take $n_2 = 0$ such that normal yielding emerges again as a possibility. Subfamily {IIaa} is similar, but not equivalent, to the only possible solutions of family {I}. Both have in common that $n_3 = 0$, and thereby imply yielding by combined tension and shear in a principal plane. However, in {I} one has the additional condition that $\sigma_3 = \sigma_1$, i.e. that one principal component in the band is equal to the principal component perpendicular to it. By way of contrast, no such condition is present in subfamily {IIaa} where all three principal stresses may be different from each other.

In summary, for a statistically homogeneous void distribution, the orientation of the band of unhomogeneous yielding is (when determined) either: (i) a principal stress direction; or (ii) lies in a principal plane, say $\mathbf{e}_1$–$\mathbf{e}_2$, and satisfies a condition of the type:

$$F + G(\sigma_1 + \sigma_2) = 0 \quad \text{AND} \quad \sigma_1 \neq \sigma_2 \tag{31}$$

where $F(\sigma, \tau)$ and $G(\tau)$ are defined through Eqs. (24) and (26). The third principal stress σ_3 (which is in the plane of the band) may be equal to one of the other two principal stresses (subfamily {I}) or not (subfamily {IIaa}). For purely hydrostatic loading, the orientation of the band is undetermined. This special case falls under subfamily {IIab}. It implies the presence of a vertex on the hydrostatic axis, see Section 5.3.

It is important to note that the above stated solutions are only *potential* ones and three factors must be considered before determining the actual band orientation. First, Eq. (24) only expresses a necessary condition. In addition, that condition is for finding extrema, not necessarily maxima. Finally, when more than one solution is possible (which is common in practice) they must be compared together to settle on the optimal band orientation.

It is equally important to note that, in writing Eq. (31), the principal stresses are not ordered. This means that, at least in theory (and as we will see in some practical cases), yielding by combined tension and shear may be possible in a principal plane other than that defined by the major and minor stresses. Whether this occurs is criterion dependent.

The effective yield criterion is thus written as:

$$\boldsymbol{\Phi}(\boldsymbol{\sigma}) = \phi(\sigma(\bar{\mathbf{n}}), \tau(\bar{\mathbf{n}})) \quad \text{where} \quad \bar{\mathbf{n}} = \underset{\mathbf{n} \in \partial \mathcal{B}}{\operatorname{argmax}}\ \phi(\sigma, \tau) \tag{32}$$

That $\boldsymbol{\Phi}$ is isotropic may be seen from the fact that $\bar{\mathbf{n}}$ only depends on the principal stresses (or their direction). This can be made more explicit since $\bar{\mathbf{n}}$ (when determined) is either parallel to a principal stress direction (normal yielding) or lies in a principal plane (yielding under combined tension and shear). In the latter case, Eq. (31) is rewritten as:

$$\tau f(\sigma) - \sigma g(\tau) + \frac{1}{2}(\sigma_1 + \sigma_2) g(\tau) = 0 \tag{33}$$

where criterion-dependent functions f and g are given by Eq. (25). Using Eq. (22), the resolved normal and shear stresses on the optimal band may be written in terms of principal stresses as: $\sigma = \bar{n}_1^2 \sigma_1 + \bar{n}_2^2 \sigma_2$ and $\tau = \bar{n}_1 \bar{n}_2 (\sigma_1 - \sigma_2)$ since $\bar{n}_3 = 0$ necessarily. An implicit equation determining the components of $\bar{\mathbf{n}}$ is then obtained from Eq. (33), which reads:

$$g \bar{n}_1^2 - f \bar{n}_1 \sqrt{1 - \bar{n}_1^2} - \frac{1}{2}\, g = 0 \tag{34}$$

For unequal principal stresses ($\sigma_1 \neq \sigma_2$), this condition hides a simpler expression in terms of the oriented angle θ ($0 \leq \theta \leq \pi/2$) between an eigenvector of $\boldsymbol{\sigma}$, say $\mathbf{e}_1$, and the orientation of the optimal band, $\bar{\mathbf{n}}$:

$$\tan 2\theta = \frac{g}{f} = \frac{\phi_{,\tau}}{\phi_{,\sigma}} \tag{35}$$

where the comma is a shorthand notation for partial derivative consistent with Eq. (25). The result in Eq. (35) implies that for a linear criterion, such as Mohr–Coulomb, the band orientation is independent of the stress state. If the intrinsic criterion is homogeneous in the stresses (e.g. elliptic criterion) then the band orientation depends on the stress state only through stress ratios. On the other hand, if ϕ is not homogeneous then the band orientation would also depend on the magnitude of the stresses. This would be expected for a criterion such as the last one listed in Table 1 or a criterion that involves transcendental functions.

5.2. Implications for failure

Potential implications for material failure may now be discussed if unhomogeneous yield criteria are used *de facto* as failure criteria. While limited, such usage is common in engineering practice. Table 2 summarizes some results. The effective (isotropic) yield criterion, which is used as a failure criterion, is listed in the second column, now fully parameterized. The first four cases are taken from Table 1. The fifth one listed is the Mohr–Coulomb criterion, which as noted above, does not emerge from some basic yield criterion of a porous material. Determining the possibility of normal or shear failure as well as the orientation and plane of

Table 2
Isotropic unhomogeneous-yield criteria, possible failure modes and their characteristics.

Type	Effective yield criterion, $\Phi = 0$	Normal failure	Shear failure	
			Orientation, θ	Plane
Rankine–Tresca	$\max\left\{\frac{\lvert\sigma\rvert}{a}, \frac{\lvert\tau\rvert}{b}\right\} = 1$	yes	0 or $\frac{\pi}{4}$	Mm
Elliptic	$\frac{\sigma^2}{a^2} + \frac{\tau^2}{b^2} = 1$	yes	$\cos 2\theta = \frac{b^2}{a^2 - b^2}\frac{\sigma_1 + \sigma_2}{\sigma_1 - \sigma_2}$	Mm or Mμ
"Cam-Clay"	$\left(\frac{\sigma}{a} - 1\right)^2 + \frac{\tau^2}{b^2} = 1$	yes	$\cos 2\theta = E - \frac{2ab^2}{a^2 - b^2}\frac{1}{\sigma_1 - \sigma_2}$	Mm
"Beams"	$\frac{\sigma^2}{a^2} + \frac{\lvert\tau\rvert}{b} = 1$	yes	$\tan 2\theta = \frac{a^2 \operatorname{sgn} s}{b(p + s\cos 2\theta)}$	Mm
Mohr–Coulomb	$\sigma \tan\varphi + \tau = c$	no	$\tan 2\theta = \frac{1}{\tan\varphi}$	Mm

failure in all cases requires technical details that go beyond the scope of this paper and will be reported elsewhere. Here, it suffices to highlight key observations.

First of all, normal failure is not predicted by the Mohr–Coulomb model. This model predicts that failure always occurs due to combined shear and tension (i) in the plane defined by the major and minor principal stresses (denoted "Mm" in the table); and (ii) with the angle θ being set by, but not equal to, the friction angle φ. This has long been known, e.g. Labuz and Zang (2012), but is worth emphasizing.

Interestingly, all other criteria predict that normal failure is possible. For shear failure, the Rankine–Tresca yield function, which is differentiable only outside of the lines $|\sigma|/a = |\tau|/b$, leads to a failure angle of either 0 (tension-dominant loading) or $\pi/4$ (shear-dominant) in a Mm plane. A key result is that, using the elliptic criterion ($a \neq b$), the orientation of the failure plane is predicted to be stress-state dependent, independent of the magnitude of the stresses. What is of particular importance is that failure may occur in a principal plane defined by the first two principal stresses, that is the major and intermediate (or middle) ones. This plane is referred to as Mμ in Table 2.

As noted above, if the criterion is not homogeneous in the stresses, the orientation of the failure plane would depend not only on the stress state but also on the magnitude of the stresses. This is the case for the "Cam–Clay" or "Beam-like" criteria. The term E in the "Cam–Clay" row refers to the value of $\cos 2\theta$ for the elliptic criterion given one row above. In the fourth row, the notations $p = \sigma_1 + \sigma_2$ and $s = \sigma_1 - \sigma_2$ were used. The possibility of failure in a Mμ plane for these two criteria is not excluded and merits study.

5.3. Formulation in terms of stress invariants

It may be of interest to express unhomogeneous yield criteria in terms of stress invariants. Unlike for homogeneous yield models, this is *not* the natural way of capturing the basic physics. However, it has the virtue of exhibiting some key features in the Haigh–Westergaard space.

Given a yield criterion in *intrinsic* form: $\Phi(\sigma, \tau) = 0$, where it is understood that σ and τ are resolved on the optimal band, first express the criterion in terms of principal stresses σ_1, σ_2, σ_3. If ordered, these will be denoted $\sigma_{\mathrm{I}} \geq \sigma_{\mathrm{II}} \geq \sigma_{\mathrm{III}}$. Since yielding cannot occur but in a principal plane, it is convenient to use the following transformations:

$$\begin{cases} \sigma = \dfrac{\sigma_1 + \sigma_2}{2} + \dfrac{\sigma_1 - \sigma_2}{2}\cos 2\theta \\ \tau = \dfrac{\sigma_1 - \sigma_2}{2}\sin 2\theta \end{cases} \tag{36}$$

with θ given by Eq. (35). Substituting the above in the yield condition gives the latter in terms of principal stresses in implicit form. When the angle θ is given explicitly in terms of principal stresses (see Table 2) it may be possible to obtain explicit expressions. Examples are reported in Table 3 for the Rankine–Tresca (RT), elliptic (E) and Mohr–Coulomb (MC) criteria. The RT and MC criteria are given in terms of ordered principal stresses because yielding must occur in the plane defined by the major and minor stresses. The elliptic criterion assumes $a \neq b$ and the expression given is *not* valid near the $\sigma_1 = \sigma_2$ axis.

Table 3
Isotropic yield criteria in intrinsic form and in terms of principal stresses or stress invariants. Lode-dependent parameters, C, D and K, L are given in text.

Type	Intrinsic form	In terms of principal stresses	In terms of invariants
	$\Phi(\sigma,\tau)=0$	$\{\sigma_1,\sigma_2,\sigma_3\}$	$\{\sigma_m,\sigma_{eq},\Theta\}$
RT	$\max\left\{\frac{\lvert\sigma\rvert}{a},\frac{\lvert\tau\rvert}{b}\right\}=1$	$\lvert\sigma_I\rvert=a$ if $\theta=0$ $\sigma_I-\sigma_{III}=2b$ if $\theta=\frac{\pi}{4}$	$\lvert\sigma_m+\frac{2}{3}\sigma_{eq}\cos\Theta\rvert=a$ $(C-D)\sigma_{eq}=3b\ ;\ \sigma_I+\sigma_{III}<2a$
E	$\frac{\sigma^2}{a^2}+\frac{\tau^2}{b^2}=1$	$\frac{(\sigma_1+\sigma_2)^2}{4(a^2-b^2)}+\frac{(\sigma_1-\sigma_2)^2}{4b^2}=1$	$\frac{\sigma_m^2}{a^2-b^2}+\frac{\sigma_{eq}^2}{K(\Theta)^2}+\frac{\sigma_m\sigma_{eq}}{L(\Theta)}=1$
MC	$\sigma\tan\varphi+\tau=c$	$(1-\sin\varphi)\sigma_I-(1+\sin\varphi)\sigma_{III}$ $=2c\cos\varphi$	$t\frac{\sigma_m}{c}+\left[\left(t+\sqrt{1+t^2}\right)C+\right.$ $\left.\left(t-\sqrt{1+t^2}\right)D\right]\frac{\sigma_{eq}}{3c}=1$

To obtain expressions in terms of the stress invariants, I_1, J_2 and J_3, the Haigh–Westergaard parameters are used:

$$\begin{cases}\sigma_m=\dfrac{1}{3}I_1\\ \sigma_{eq}=\sqrt{3J_2}\\ \cos 3\Theta=\dfrac{3\sqrt{3}}{2}\dfrac{J_3}{J_2^{\frac{3}{2}}}\end{cases}\tag{37}$$

where σ_m is the mean normal stress (hydrostatic pressure), σ_{eq} is the equivalent stress and Θ is the Lode angle (not to be confused with the orientation θ of the optimal band). To this end, the principal stresses are expressed in terms of the above parameters using:

$$\begin{cases}\sigma_1=\sigma_m+\dfrac{2}{3}\sigma_{eq}\cos\Theta\\ \sigma_2=\sigma_m+\dfrac{2}{3}\sigma_{eq}\cos\left(\Theta-\dfrac{2\pi}{3}\right)\\ \sigma_3=\sigma_m+\dfrac{2}{3}\sigma_{eq}\cos\left(\Theta+\dfrac{2\pi}{3}\right)\end{cases}\tag{38}$$

Then substituting in the yield criteria expressed in terms of principal stresses provides the desired expressions, after rearrangement, in terms of invariants. Examples are provided in the last column of Table 3. In general, a and b may be arbitrarily ordered but physics demands $a\geq b$, a case we restrict attention to.

For the elliptic criterion,

$$K(\Theta)=3b\sqrt{\frac{a^2-b^2}{(C-D)^2a^2+4CDb^2}},\qquad L(\Theta)=\frac{3(a^2-b^2)}{2(C+D)}\tag{39}$$

where all Lode-dependence enters through $C=\cos\Theta$ and $D=\cos\left(\Theta+\frac{2\pi}{3}\right)$, which also appear in the other criteria. Again, the expression given is *not* valid near the hydrostatic axis. Also, with $t\equiv\tan\varphi$, an alternative expression for the MC criterion in the principal stress space is:

$$\left(t+\sqrt{1+t^2}\right)\sigma_I-\left(t-\sqrt{1+t^2}\right)\sigma_{III}=2c\tag{40}$$

which was used to obtain the expression in the last column of the table.

The complexity of the expressions in terms of principal stresses or invariants hints at the fact that neither are the most natural space for capturing the physics of unhomogeneous yielding. For other criteria included in Table 2 but not in Table 3, it is not possible to obtain explicit expressions, even though the intrinsic expressions are relatively simple. On the other hand, obtaining the yield stress for as simple a loading as uniaxial tension is not straightforward using the intrinsic form (except for the RT criterion). The expression in terms of principal stresses may be used to that end.

Fig. 3 illustrates key features. The highly idealized Rankine–Tresca criterion captures key features of unhomogeneous yielding, namely: (i) For low amounts of superposed pressure, the octahedral section of the yield locus is Tresca-like, Fig. 3b. This is

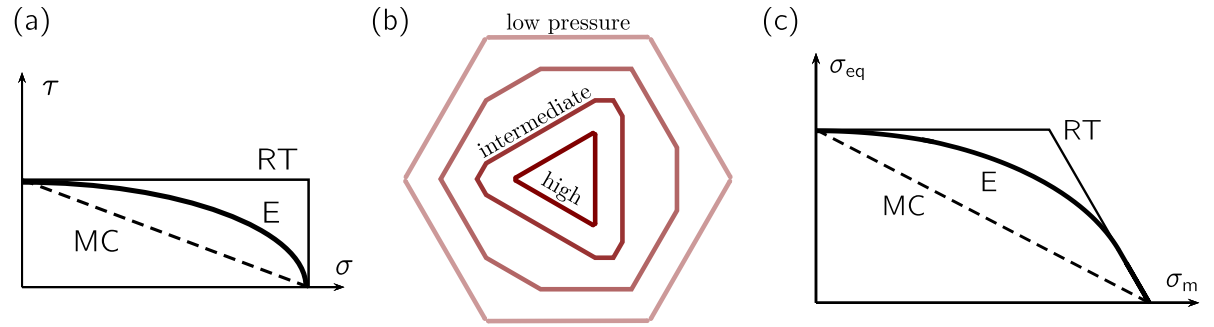

Fig. 3. Surfaces of unhomogeneous yielding (a) intrinsic; (b) octahedral; (c) meridional.

a remarkable feature given that the microscale yield criterion is putatively[8] von Mises. (ii) For large amounts of pressure, the octahedral section is Rankine-like, Fig. 3b. (iii) For intermediate pressures, there is a gradual transition from a hexagonal prism (pressure-independent Tresca-like effective behavior) to a right cone with a triangular base and an apex on the hydrostatic axis. In transition, the octahedral section is an irregular nonagon. Two examples are shown in Fig. 3b.

Obviously, the above features have to do with (unhomogeneous) yielding being controlled by the maximum shear stress at low pressure and by the maximum normal stress at high pressure. The Tresca-like octahedral section is an essential characteristic of any unhomogeneous-yield criterion, even if the pore-free matrix were governed by J_2 flow theory. This is much different from some recent "porous Tresca" criteria where the matrix obeys a Tresca criterion, e.g. Cazacu et al. (2014). In the latter case, the overall J_3 dependence essentially results from that assumed in the matrix. That is not the case for unhomogeneous yielding where J_3 dependence is purely emergent behavior.

Details aside, such features hold for the other two criteria (elliptic and MC) as well as any physics-based criterion, e.g. Torki et al. (2015). The low-pressure octahedral section of the elliptic criterion may look as a hexagon but with curved regions near tension states. One other key difference is that the size of the section shrinks as the superposed pressure increases. The MC surface octahedral section has an irregular shape, as is well known. All sections in Fig. 3b are for the RT criterion.

What is of particular importance is the presence of a corner on the hydrostatic axis, Fig. 3c. This is a *universal* feature of the class of (isotropic) unhomogeneous-yield criteria derived here. Physically, this indicates the presence of regions of extreme curvature on the hydrostatic axis, as confirmed numerically (Keralavarma, 2017; Torki et al., 2021).

Expressions of the yield criteria in terms of invariants may or may not be valid under pure pressure loading. For instance, that of the elliptic criterion is not, because the formula used for the optimal band orientation is no longer valid in that case, as θ is undetermined. What is plotted in that case is the envelope of intrinsic yield surfaces parameterized by θ. The yield pressure $\sigma_{\rm m}^{\rm U}$, to be sure, is always obtained from the intrinsic yield function as: $\Phi(\sigma_{\rm m}^{\rm U}, 0) = 0$, which gives unequivocally $\sigma_{\rm m}^{\rm U} = a$ (identified with $c/\tan\varphi$ for the MC criterion).

In meridional sections, the MC surface has an unphysical corner on the $\sigma_{\rm eq}$ axis. The values of the zero-pressure yield stresses are the same for the RT and elliptic criteria for all Lode angles. That is not the case for the MC criterion, except for shear states ($\Theta = \pi/6$), which is the case shown in Fig. 3c.

5.4. A fundamental result

The above discussion ignores the effect of physically meaningful internal parameters, such as porosity. In actuality, the model coefficients a and b are porosity-dependent.

One estimate that has long been known is the yield pressure of a porous material (Hill, 1950):

$$\sigma_{\rm m}^{\rm H} = -\frac{2}{3}\bar{\sigma}\ln f \tag{41}$$

where $\bar{\sigma}$ is the matrix yield stress and f the porosity. But an inquiry into the yield stress of a porous material under a loading path is incomplete until it specifies the mode of yielding, homogeneous versus unhomogeneous. The above estimate, which is the exact solution for a hollow sphere under pure pressure loading, is obviously for homogeneous yielding.

An estimate of the yield pressure for the unhomogeneous mode, $\sigma_{\rm m}^{\rm U}$, may be determined as follows. For a random distribution of voids, the orientation of the yield band is undetermined. This implies the presence of a corner on the hydrostatic axis. The value

[8] The RT criterion does not emerge from rigorous homogenization. However, the TBL criterion in Table 1 does, and has a Tresca-like shape on the π-plane at sufficiently low pressure.

of $\sigma_{\rm m}^{\rm U}$ is, however, determined by the yield traction normal to the band, equal to the applied pressure, as inferred from the solution of Benzerga and Leblond (2014), specialized to equiaxed voids:

$$\sqrt{3}\frac{\sigma_{\rm m}^{\rm U}}{\bar{\sigma}} = 2 - \sqrt{1+3f^{\frac{4}{3}}} + \ln\frac{1+\sqrt{1+3f^{\frac{4}{3}}}}{3f^{\frac{2}{3}}} + \frac{f-3f^{\frac{1}{3}}+2}{3f^{\frac{1}{3}}} \tag{42}$$

Comparison between the two estimates (Fig. 4) shows that they are remarkably close to each other over the *entire* range of porosity for $f > 0.01$, Fig. 4b. In the low-porosity regime, Fig. 4a, we have $\sigma_{\rm m}^{\rm U} > \sigma_{\rm m}^{\rm H}$, as expected if the band thickness remains comparable with the void size. There is no general principle stating that homogeneous yielding should prevail for dilute porosity. One can only state that insofar as the band thickness does not exceed the void size, homogeneous yielding would prevail for low porosities. The issue merits further analysis.

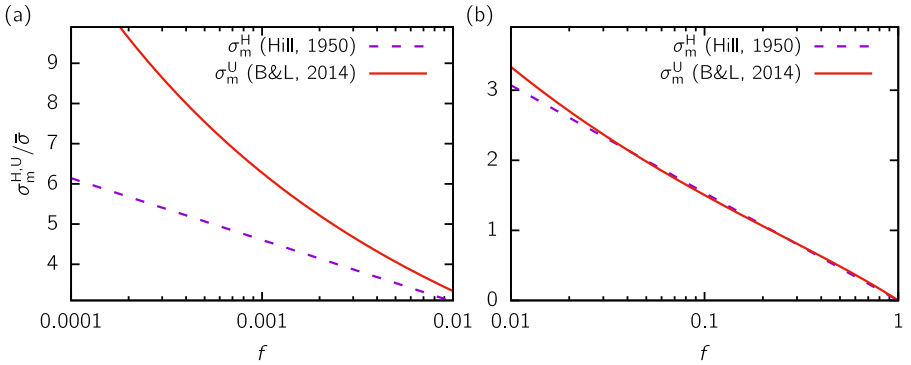

Fig. 4. Pressure for homogeneous yielding, $\sigma_{\rm m}^{\rm H}$ in Eq. (41), and unhomogeneous yielding, $\sigma_{\rm m}^{\rm U}$ in Eq. (42), versus porosity. (a) Low porosity regime. (b) Moderate to high porosity regime.

When the above result for the $f > 0.01$ regime is combined with an estimate for yielding in shear (Drucker, 1966), a fundamental result is obtained in that the entire unhomogeneous yield locus is essentially interior to its homogeneous counterpart for shearing states, Fig. 5b. Indeed, the two conditions:

$$\sigma_{\rm m}^{\rm U} \approx \sigma_{\rm m}^{\rm H} \quad \text{and} \quad \sigma_{\rm eq}^{\rm U} < \sigma_{\rm eq}^{\rm H} \tag{43}$$

combined with the convexity requirement for each surface leads to the stated result (recall that on the $\sigma_{\rm m}$-axis the tangent to the HY surface is vertical whereas the slope of the UY surface is $-\sqrt{3}$). In terms of the Lode angle Θ, this means that the $\Theta = \pi/6$ section of the yield locus is essentially dominated by unhomogeneous yielding. This is a remarkable finding.

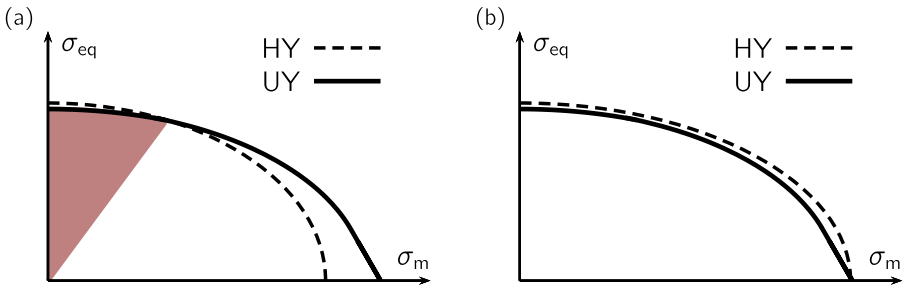

Fig. 5. Yield surfaces for "shearing states" in the absence of strain hardening. (a) Low porosity regime. (b) Moderate to high porosity regime.

On the other hand, for sufficiently low porosity, say below 0.001, one may still infer from the inequality in Eq. (43) and the presence of a corner on the surface for unhomogeneous yielding that the latter would dominate for a significant portion of the low triaxiality regime (shown shaded in Fig. 5a). In all cases, it is emphasized that these predictions are valid in the absence of strain hardening. The effect of the latter will be analyzed in more detail in Section 7.

6. General theory with internal variables

The general theory presumes a *finite* number of unhomogeneous yield systems. It is therefore anisotropic. This anisotropy, to be sure, is beyond that which may result from considering non-spherical pore shapes or characterize plastic flow in the matrix itself. To each yield system corresponds a yield condition in terms of the resolved normal and shear stresses, of the type introduced in Section 4. Each yield condition is parameterized, e.g. using a and b in the criteria listed in Table 2. In a phenomenological approach, these parameters are structureless. Furthermore, they need not be the same for all systems in a multi-yield system analysis. In a micromechanical approach, however, the a's and b's entering a given yield condition are parametric functions of internal variables, which naturally arise in the analysis as geometrical or topological descriptors of the pores and their spatial distribution. Furthermore, analytical expressions of such functions ought to be derivable from first principles, thereby considerably reducing the number of parametric functions, ideally with no parameters at all.

6.1. Internal variables

In porous material plasticity, porosity-related internal parameters naturally emerge when solving a problem of the type posed in Section 3.1. A complete theory would involve the lengths and orientations of the pore axes, as well as the pore spacings relative to some frame. Given these, a void volume fraction, f, is introduced. Not only is f the sole relevant internal variable in the limit of isotropic response but it also evolves in accordance with a universal principle, irrespective of anisotropy. It is thus retained in all descriptions.

For homogeneous yielding, Madou et al. (2013) introduced, in addition to f, a quadratic form $\mathcal{W}$ with matrix $\mathbf{W}$ the eigenvalues of which are related to the (mean) pore lengths and the eigenvectors of which are the (mean) pore axes. The void spacing plays no role in their description[9] nor does it enter any homogeneous yield model in general.

For unhomogeneous yielding, f and $\mathbf{W}$ are important descriptors but the spatial distribution of pores is paramount and its characterization introduces new internal variables. In general, with each yield system k ($1 \leq k \leq n$) are associated a normal $\mathbf{n}^k$ and a scalar λ^k, the latter representing the mean in-plane pore spacing relative to the out-of-plane pore spacing. Alternatively, one may introduce a form $\mathcal{L}$ with matrix $\boldsymbol{\Lambda}$, which would be the counterpart of $\mathbf{W}$ for the void distribution. This would be appropriate for an "ellipsoidal symmetry" for the void arrangement (Willis, 1977; Ponte Castañeda and Willis, 1995).

Several characterizations of the spatial pore distribution are *a priori* possible. Whichever way is used, one should recognize that not only metric descriptors are needed but also topological ones. To this end, it is useful to classify pore distributions using three general categories: random, ordered or clustered.

In the present context, by random distribution we mean something very specific, namely that for which the pore centers are distributed according to a Poisson process. In that sense, no distribution can exactly be random since, by the excluded volume argument, a finite porosity system would be incompatible with a Poisson process. Nevertheless, the random case in that sense is a useful limit for which $n \to \infty$ and the general theory reduces to a simpler isotropic one. In the isotropic limit, the optimal band orientation is either a principal stress direction or that given by Eq. (35) and the associated relative pore spacing λ is necessarily unity.

In order to characterize ordered or clustered pore distributions, one needs to identify the total number n of yield systems and, for each system, its orientation $\mathbf{n}^k$ and the associated relative pore spacing, λ^k. As alluded to as early as Section 2.1, a yield system is a band of dense pore packing. If the distribution were ordered, determining planes of dense pore packing would be straightforward. If the distribution is clustered, one practical way would be to construct its Dirichlet tessellation and determine such planes using the line intercept method. Clearly, this method is suggested to make a tighter contact with experimental measurements, since quantitative image analysis is nowadays routine. Otherwise, the user may specify as many yield systems as desired for quantifying the uncertainties associated with actual pore distributions.

On the physical meaning of multiple yield systems

Fig. 6a shows the spatial arrangement of holes in plasticine after plastic deformation (McClintock, 1968). The figure illustrates a state of unhomogeneous yielding being clearly active. The sketch in Fig. 6b illustrates potential yield systems. The scale at which the phenomenon is resolved is obviously an issue, but that is no different than identifying slip systems in a plastically deformed crystal volume. If the resolution is that of a few mean void spacings, it is clear that multiple systems may be at play. The present theory attempts to account for just that.

[9] The elementary cell considered by Madou et al. (2013) is an ellipsoid containing a confocal ellipsoidal pore, such that the pore spacings are actually constrained by the pore dimensions and not independent. This has no effect in their case but would have a tremendous effect in any unhomogeneous yield model.

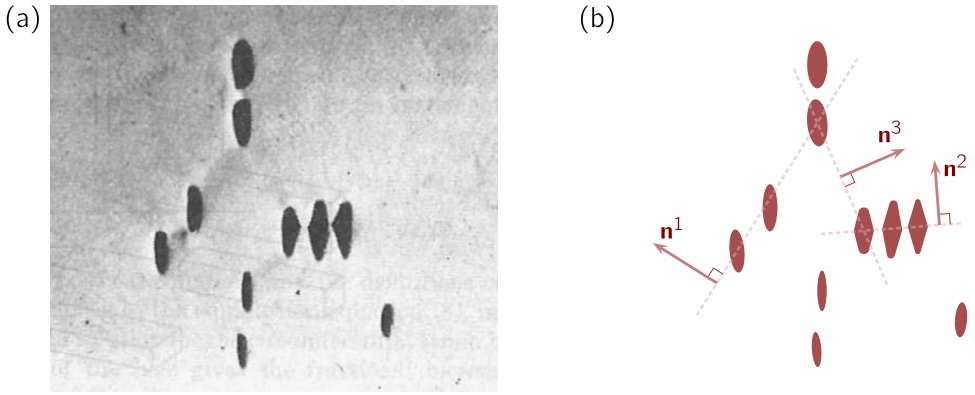

Fig. 6. (a) Holes in a state of unhomogeneous yielding, after McClintock (1968). (b) Identification of potential yield systems.

6.2. Synopsis

We adopt an eulerian setting to describe the general constitutive relations of an elasto-plastic porous material. The total rate of deformation is additively decomposed into elastic and plastic parts:

$$\mathbf{D} = \mathbf{D}^{\mathrm{e}} + \mathbf{D}^{\mathrm{p}} \tag{44}$$

with

$$\mathbf{D}^{\mathrm{e}} = \mathbb{C} : \overset{\triangledown}{\boldsymbol{\sigma}} \tag{45}$$

where $\mathbb{C}$ denotes an effective elastic compliance tensor and $\triangledown$ a corotational rate. $\mathbb{C}$ may be taken to depend on void volume fraction f to account for poroelasticity where relevant.

The plastic part is given by:

$$\mathbf{D}^{\mathrm{p}} = \dot{\gamma}^{\mathrm{H}} \frac{\partial \boldsymbol{\Phi}^{\mathrm{H}}}{\partial \boldsymbol{\sigma}} + \sum_{k=1}^{n} \dot{\gamma}^{k} \frac{\partial \phi^{k}}{\partial \boldsymbol{\sigma}} \tag{46}$$

where $\boldsymbol{\Phi}^{\mathrm{H}}$, ϕ^{k} are activation functions for homogeneous and unhomogeneous yielding, respectively, and $\dot{\gamma}^{\mathrm{H}}$, $\dot{\gamma}^{k}$ are corresponding plastic multipliers. The general forms of the yield conditions are:

$$\boldsymbol{\Phi}^{\mathrm{H}}(\boldsymbol{\sigma}; \boldsymbol{\alpha}^{\mathrm{H}}) \leq 0 \qquad \boldsymbol{\alpha}^{\mathrm{H}} \equiv \{f, \mathbf{W}\} \tag{47}$$

for homogeneous yielding and

$$\phi^{k}(\boldsymbol{\sigma}; \boldsymbol{\alpha}^{k}) \leq 0 \qquad \boldsymbol{\alpha}^{k} \equiv \{f, \mathbf{W}, \mathbf{n}^{k}, \lambda^{k}\} \tag{48}$$

for unhomogeneous yielding on system k, where the sets $\boldsymbol{\alpha}^{\mathrm{H}}$ and $\boldsymbol{\alpha}^{k}$ ($k = 1 \cdots n$) of internal variables introduced in the previous section have been used where appropriate.

Where convenient, we shall use the set $\mathcal{S}$ of superscripts: $\mathcal{S} = \{\mathrm{s} \mid \mathrm{s} = \mathrm{H} \text{ or } \mathrm{s} = 1, \ldots, n\}$ to refer to various *processes* of yielding. The surfaces $\phi^{\mathrm{s}}(\boldsymbol{\sigma}; \boldsymbol{\alpha}^{\mathrm{s}}) = 0$ (with $\phi^{\mathrm{H}} \equiv \boldsymbol{\Phi}^{\mathrm{H}}$) denote the portions of the current yield surface in stress space, and $\partial \phi^{\mathrm{s}} / \partial \boldsymbol{\sigma}$ denotes the outward normal to each portion. In writing Eq. (46) one could subsume the first term under the sum, but we prefer not to do this in order to emphasize that there are many potential systems for unhomogeneous yielding but only *one process* of homogeneous yielding with corresponding surface $\boldsymbol{\Phi}^{\mathrm{H}} = 0$.

The conditions under which a yield process is active, $\dot{\gamma}^{\mathrm{s}} > 0$, or inactive, $\dot{\gamma}^{\mathrm{s}} = 0$, are based on the usual Kuhn–Tucker relations, namely:

$$\dot{\gamma}^{\mathrm{s}} \geq 0, \qquad \phi^{\mathrm{s}} \leq 0, \qquad \dot{\gamma}^{\mathrm{s}} \phi^{\mathrm{s}} = 0 \tag{49}$$

Physics imposes that the process of homogeneous yielding, $\mathrm{s} = \mathrm{H}$, and any system of unhomogeneous yielding, $\mathrm{s} = k, k = 1 \cdots n$, are mutually exclusive. Hence, the constraint

$$\forall k, \quad \dot{\gamma}^{\mathrm{H}} \dot{\gamma}^{k} = 0 \tag{50}$$

also applies.[10] On the other hand, multiple systems of unhomogeneous yielding may be concurrently active, as illustrated in Fig. 6. For active processes, the magnitudes of $\dot{\gamma}^{\mathrm{s}}$ are determined using the consistency condition $\dot{\phi}^{\mathrm{s}} = 0$. Iterative methods may be employed to this end (Anand and Kothari, 1996).

[10] Unless the elementary volume contains many voids such that regions are in a state of unhomogeneous yielding and others in a state of homogeneous yielding. This is obviously a resolution issue.

An appropriate choice for Φ^{H} is any Gurson-like yield function that would result from solving the problem defined by Eq. (15) in Section 3.1 using $\mathbf{v} \in \mathcal{K}^{\mathrm{H}}$. A most general form for plastically isotropic matrices is that of Madou and Leblond (2012).

As for unhomogeneous yielding, the activation function is the same for all systems, i.e.,

$$\phi^k(\boldsymbol{\sigma}; \boldsymbol{\alpha}^k) = \phi(\sigma^k, \tau^k; \boldsymbol{\alpha}^k) \tag{51}$$

where it is emphasized that stress dependence enters only through the resolved normal stress, σ^k, and resolved shear stress, τ^k, defined as in Eq. (22) using $\mathbf{n}^k$ instead of $\mathbf{n}$. At present, rigorous solutions, e.g. Benzerga and Leblond (2014), are only available when $\mathbf{n}^k$ is an eigenvector of $\mathbf{W}$. This corresponds to situations where the pore and system orientations coincide, which obviously cannot be satisfied under multi-activation conditions. The development of more general yield functions merits further efforts.

In an evolution problem, each yield surface $\phi^s = 0$ evolves as a result of hardening and softening processes. A simple approach for incorporating strain hardening is that of Gurson (1977), which has serious shortcomings for shearing states. This will be considered in some detail in Section 7. Here, focus is placed on the evolution of internal variables when unhomogeneous yielding is active. This evolution generally induces softening.

The evolution of the void volume fraction results from plastic incompressibility of the matrix (Gurson, 1977):

$$\dot{f} = (1 - f)\,\mathrm{tr}\,\mathbf{D}^{\mathrm{p}} \tag{52}$$

Under finite deformations, the spatial pore distribution evolves thereby affecting current values of both the orientation $\mathbf{n}^k$ of the yield system and the associated relative pore spacing, λ^k. Using standard kinematical relations in terms of the deformation gradient $\mathbf{F}$, the current orientation is obtained as:

$$\mathbf{n}^k = \frac{\mathbf{F}^{-T}\mathbf{n}_0^k}{|\mathbf{F}^{-T}\mathbf{n}_0^k|} \tag{53}$$

and the current relative spacing is, under certain conditions (see Appendix E):

$$\lambda^k = \frac{\lambda_0^k}{\sqrt{\det \mathbf{F}}}\left(\mathbf{n}^k \cdot \mathbf{B}\mathbf{n}^k\right)^{\frac{3}{4}} \tag{54}$$

where $\mathbf{n}_0^k$ and λ_0^k denote initial values and $\mathbf{B}$ is the left Cauchy–Green deformation tensor. Eq. (53) simply states how an *immaterial* unit vector transforms. On the other hand, a variant of Eq. (54) was derived by Leblond and Mottet (2008) based on (material) area and volume change and is therefore predicated on a certain type of pore distribution, namely the ordered category. Eq. (54) is *not* valid for a random pore distribution. In that case, the initial isotropy is persistent and one rigorously has:

$$\forall k, \quad \lambda^k = 1 \qquad \text{random case} \tag{55}$$

For clustered pore distributions, a proper evolution equation for λ^k is lacking. This alone merits study.

The evolution of the lengths and axes of the pores, as embodied in matrix $\mathbf{W}$, requires a rate equation for the latter. A straightforward kinematical relation connects the said evolution to the average strain-rate and rotation-rate of the pores, $\mathbf{D}^{\mathrm{v}}$ and $\boldsymbol{\Omega}^{\mathrm{v}}$, respectively:

$$\dot{\mathbf{W}} = -\mathbf{W}\left(\mathbf{D}^{\mathrm{v}} + \boldsymbol{\Omega}^{\mathrm{v}}\right) - \left(\mathbf{D}^{\mathrm{v}} + \boldsymbol{\Omega}^{\mathrm{v}}\right)^T \mathbf{W} \tag{56}$$

Madou et al. (2013) derived expressions for $\mathbf{D}^{\mathrm{v}}$ and $\boldsymbol{\Omega}^{\mathrm{v}}$ for homogeneous yielding. The general structure of tensors $\mathbf{D}^{\mathrm{v}}$ and $\boldsymbol{\Omega}^{\mathrm{v}}$ in the case of unhomogeneous yielding is elicited in Appendix F. Both $\mathbf{D}^{\mathrm{v}}$ and $\boldsymbol{\Omega}^{\mathrm{v}}$ are related to $\mathbf{D}^{\mathrm{p}}$ via concentration tensors $\mathbb{C}^{\mathrm{s}}$ and $\mathbb{R}^{\mathrm{s}}$, such that:

$$\mathbf{D}^{\mathrm{v}} = \sum_{\mathrm{s}\in S} \dot{\gamma}^{\mathrm{s}}\mathbb{C}^{\mathrm{s}} : \frac{\partial \phi^{\mathrm{s}}}{\partial \boldsymbol{\sigma}} \qquad \boldsymbol{\Omega}^{\mathrm{v}} = \boldsymbol{\Omega} + \sum_{\mathrm{s}\in S} \dot{\gamma}^{\mathrm{s}}\mathbb{R}^{\mathrm{s}} : \frac{\partial \phi^{\mathrm{s}}}{\partial \boldsymbol{\sigma}} \tag{57}$$

where $\boldsymbol{\Omega} = \mathrm{skw}(\dot{\mathbf{F}}\mathbf{F}^{-1})$ is the continuum spin. The concentration tensors can be formulated rigorously based on the peculiar kinematics of unhomogeneous yielding, as described in Section 2.1. This is in contrast with the derivations of $\mathbf{D}^{\mathrm{v}}$ and $\boldsymbol{\Omega}^{\mathrm{v}}$ by Madou et al. (2013), which unavoidably required a series of heuristics.

To illustrate the derivation procedure for $\mathbf{D}^{\mathrm{v}}$, consider a material with spheroidal pores under axisymmetric triaxial tension. If the principal axes of loading are parallel to the pores then a potential system of unhomogeneous yielding is normal to the major principal stress, such that its orientation $\mathbf{n}$ coincides with the pore axis. By symmetry, the rotation rate of the pore is nil and the velocity of a point on the pore's boundary is given by: $\mathbf{v} = \mathbf{D}^{\mathrm{v}}\mathbf{x}$. If the thickness of the band of unhomogeneous yielding is identified with the pore height, h, as conjectured by Benzerga (2002),[11] then the pore's top and bottom are intercepted by the elastically unloaded zones, here modeled as rigid. Therefore, at the poles, only the axial velocity is nonzero, $v = D^{\mathrm{v}}_{nn}h = D_{nn}H$ (no sum on n) with H the height of the elementary volume, also identified with the pore spacing normal to the band. Thus, one has

$$D^{\mathrm{v}}_{nn} = \frac{1}{c}D^{\mathrm{p}}_{nn} \qquad \text{no sum on } n \tag{58}$$

[11] To date, this conjecture has not been falsified in the context of an *evolution problem*.

where $c \equiv h/H$ is the band volume fraction; see Section 2.1. From plastic incompressibility of the matrix material:

$$D^{\mathrm{v}}_{ii} = \frac{1}{f} D^{\mathrm{p}}_{ii} \tag{59}$$

one then gets the transverse component (i.e. parallel to the band) as:

$$D^{\mathrm{v}}_{mm} = \frac{1}{2}\left[\frac{1}{f} - \frac{1}{c}\right] D^{\mathrm{p}}_{nn} \tag{60}$$

It is thus seen that the constraint of unhomogeneous yielding, supplemented with incompressibility, entirely determines the strain rate of the pore (to the extent that a point definition of $\mathbf{D}^{\mathrm{v}}$ is sufficient) in terms of the overall plastic strain rate (recall that in the opening mode, only $D^{\mathrm{p}}_{nn} = \dot{\epsilon}$ is nonzero). Eqs. (58) and (60) lead to Benzerga (2002)'s evolution equation for the pore aspect ratio, w:

$$\frac{\dot{w}}{w} = D^{\mathrm{v}}_{nn} - D^{\mathrm{v}}_{mm} = \left[\frac{3}{2c} - \frac{1}{2f}\right]\dot{\epsilon} \tag{61}$$

In terms of the concentration tensors entering Eq. (57), $\mathbb{R} = 0$ while the few nonzero components of $\mathbb{C}$ involve c and f as per Eqs. (58) and (60). It is shown elsewhere how general expressions for $\mathbb{C}$ and $\mathbb{R}$ are obtained. Also, see Appendix F for their general structure.

6.3. Anticipated features

With a yield function having the form of Eq. (51) the contribution of unhomogeneous yielding to the rate of deformation has a mean part obtained from Eq. (46) as:

$$\mathrm{tr}\,\mathbf{D}^{\mathrm{p}} = \sum_{k=1}^{n} \dot{\gamma}^k \frac{\partial \phi}{\partial \sigma^k} \tag{62}$$

and a deviatoric part given by

$$\mathbf{D}^{\mathrm{p}\prime} = \sum_{k=1}^{n} \dot{\gamma}^k \left[\frac{\partial \phi}{\partial \sigma^k}\left(\mathbf{n}^k \otimes \mathbf{n}^k - \frac{1}{3}\mathbf{I}\right) + \frac{1}{2}\frac{\partial \phi}{\partial \tau^k}\left(\mathbf{n}^k \otimes^{\mathrm{s}} \mathbf{m}^k\right)\right] \tag{63}$$

where $\mathbf{I}$ denotes the identity tensor and $\mathbf{m}^k$ a unit vector in the direction of resolved shear. The above two relations are valid when $\dot{\gamma}^{\mathrm{H}} = 0$. Thus, during unhomogeneous yielding all dilation is due to the normal stress dependence of yielding whereas $\mathbf{D}^{\mathrm{p}\prime}$ is affected by the shear as well as the normal stress dependence. By way of comparison, for homogeneous yielding ($\dot{\gamma}^{\mathrm{H}} \neq 0$) the above apportioning would read:

$$\mathrm{tr}\,\mathbf{D}^{\mathrm{p}} = \dot{\gamma}^{\mathrm{H}} \frac{\partial \boldsymbol{\Phi}^{\mathrm{H}}}{\partial \sigma_{\mathrm{m}}} \tag{64}$$

$$\mathbf{D}^{\mathrm{p}\prime} = \frac{3}{2}\frac{\dot{\gamma}^{\mathrm{H}}}{\sigma_{\mathrm{eq}}} \frac{\partial \boldsymbol{\Phi}^{\mathrm{H}}}{\partial \sigma_{\mathrm{eq}}} \boldsymbol{\sigma}' \tag{65}$$

assuming an isotropic $\boldsymbol{\Phi}^{\mathrm{H}}$ with σ_{m} and σ_{eq} as defined in Section 5.3

With the above as basis, and for problems with evolving porosity, it is edifying to illustrate the strain-dependence of the void volume fraction, under predominately tensile loadings, if a Gurson-like yield function is used for homogeneous yielding and, say an elliptic function for unhomogeneous yielding. The void volume fraction would then exhibit *exponential* versus *linear* growth during homogeneous versus unhomogeneous yielding. Yet, the rate of growth would be much faster in the linear growth regime, Fig. 7. This example illustrates the significance of unhomogeneous yielding as an effective dilation-driving mechanism.

Next, examine the potential effect of the spatial pore distribution, once again in an evolution problem. Consider the two extremes of order and randomness. An essential attribute of an ordered distribution is deformation induced anisotropy. An essential attribute of a random distribution is persistent isotropy. This contrast renders predictions of order versus randomness that are far less intuitive than commonly reported. For an ordered distribution, the induced anisotropy is embodied in Eq. (54), which leads to an increase in λ^k in tension as pores would come closer together within the potential band, hence favoring linkup or coalescence. On the other hand, the number of potential yield systems is finite, eventually reduced to one set by the initial pore arrangement. By way of contrast, the persistent isotropy of a random distribution (i.e. $\lambda^k = 1$) would delay unhomogeneous yielding (and subsequent pore linkup) while the potentiality of band orientation would favor it. For a random distribution there is, therefore, competition between the invariability of the mean pore spacing (a consequence of persistent isotropy) and the availability of an infinite number of yield systems. As a result, whether a random distribution would lead to more softening or weakening is generally unsettled and requires analysis. We know even less of how the more realistic clustered distributions would play out.

At this junction, it is appropriate to revisit a basic premise in deriving the much useful results of Section 5. If internal variables were accounted for, which in the isotropic limit would essentially reduce to f, the extremum problem of Eq. (23) would have to be reformulated as:

$$\boldsymbol{\Phi}(\boldsymbol{\sigma}; f) = \max_{\mathbf{n}\in\partial\mathcal{B}} \phi(\sigma(\mathbf{n}), \tau(\mathbf{n}); \boldsymbol{\alpha}(\mathbf{n})) \tag{66}$$

with the obvious consequence that, in principle if not in practice, the optimal band orientation $\bar{\mathbf{n}}$ in Eq. $(32)_2$ would depend on f. For dilute pore distributions, the correction is expected to be small. However, for large porosities the dependence of $\bar{\mathbf{n}}$ upon f would merit a separate analysis.

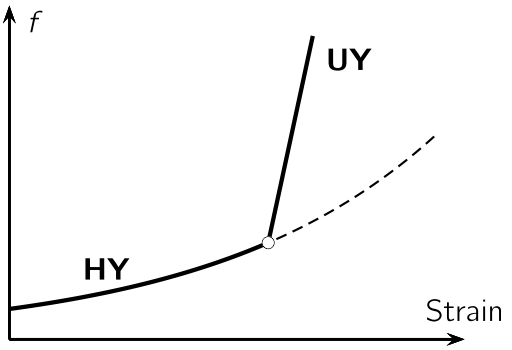

Fig. 7. Void volume fraction versus plastic strain.

6.4. Analogy with crystal plasticity

The general anisotropic theory of unhomogeneous yielding has striking similarities with crystal plasticity. The notion of yield/flow system is akin to a slip/twin system. Such systems are given and not predicted. As a result, both theories result in multisurface representations. In particular, the presence of corners in the effective yield surface introduces difficulties in numerical implementations in the rate-independent case. Advantage may be derived from progress gained in crystal plasticity in that respect, e.g. Anand and Kothari (1996).

If slip systems were at random and not crystallographically determined a Tresca criterion would emerge as the isotropic limit of crystal plasticity. In the theory of unhomogeneous yielding, this is recovered as a special case whereby the basic yield condition only depends on the resolved shear stress. Furthermore, the problem of homogenizing dislocation plasticity to infer hardening laws directly is wide open. Thus, in crystal plasticity hardening laws are heuristic, just like in porous material plasticity.

There are essential differences in the structure of the two sets of constitutive relations. In crystal plasticity, slip systems emerge from the atomic structure. In the theory of unhomogeneous yielding, flow systems come from the mere presence of voids. There is no underlying lattice per se, only a fictitious reference lattice.

An essential feature of unhomogeneous yielding is the dependence upon the resolved normal stress. When there is such dependence in crystal plasticity (non-Schmid effects) non-associative flow is typically considered. This is not the case here where normality is always obeyed overall once assumed at the micro-scale.

The isotropic version of the present theory emerges from rigorous homogenization of the “ensemble-averaging” type with a Tresca-like behavior being recovered as a trivial limit. But the overall behavior may rightly be referred to as a Rankine–Tresca behavior.

Finally, while hardening laws are heuristic, softening laws are inherent to the theory and derived from micromechanics.

7. Strain hardening

Attention is limited to isotropic hardening. Insofar as porosity evolution is affected by the local flow stress distribution, whether the latter is affected by long-range interactions, as would arise in kinematic hardening, would have little effect, if any, under monotonic loading.

7.1. Heuristic formulation

We begin with the general formulation of Section 6.2 and replace, wherever it appears, the constant yield stress with the current flow stress of the matrix $\bar{\sigma}$. The yield conditions (47) and (51) would then read: $\Phi^{\mathrm{H}}(\boldsymbol{\sigma};\boldsymbol{\alpha}^{\mathrm{H}},\bar{\sigma}) \leq 0$ and $\phi^k(\boldsymbol{\sigma};\boldsymbol{\alpha}^k,\bar{\sigma}) \leq 0$ per system k. The flow stress is evaluated at some effective strain measure, ϵ^*, the evolution of which needs to be formulated. One way consists of identifying the overall plastic dissipation, $\sigma_{ij}D^{\mathrm{p}}_{ij}$, with that of a fictitious medium having the same porosity but uniformly hardened, wherever plastic flow occurs, up to the strain ϵ^*, that is:

$$c(1-f_b)\bar{\sigma}(\epsilon^*)\dot{\epsilon}^* = \boldsymbol{\sigma} : \mathbf{D}^{\mathrm{p}} \tag{67}$$

Here, $f_b = f/c$ denotes the porosity inside the band and c, as above, the band volume fraction. Eq. (67) is general enough to encompass both homogeneous and unhomogeneous yielding. In the former case, it suffices to take $c = 1$ (plastic flow fills the entire cell) to recover Gurson’s identity.

This leads to a single-parameter representation of hardening in the porous material. Obviously, this representation does not account for the true microscopic state of hardening, which is heterogeneous in the matrix. It does account, however, for the contribution to hardening of the hydrostatic component of the loading. It is emphasized that the hardening parameter ϵ^* is different from the effective plastic strain in the matrix, which does not enter the constitutive framework.

To bring focus, take for $\Phi^{\mathrm{H}} = \Phi^{\mathrm{Gur}}(\sigma_{\mathrm{eq}}, \sigma_{\mathrm{m}}; f, \bar{\sigma})$ Gurson's yield function (1977) and take for unhomogeneous yielding an isotropic yield function $\Phi^{\mathrm{U}}(\sigma, \tau; f, \bar{\sigma})$ with τ and σ resolved on the optimal band. An adequate choice would be

$$\Phi^{\mathrm{U}}(\sigma, \tau; f, \bar{\sigma}) = \left(\frac{\sigma}{a\bar{\sigma}}\right)^2 + \left(\frac{\tau}{b\bar{\tau}}\right)^2 - 1 = 0 \tag{68}$$

where $\bar{\tau} = \bar{\sigma}/\sqrt{3}$. Also, a and b are functions of the void volume fraction given by:

$$\begin{cases} a(f) = -\dfrac{2}{3}\ln f \\ b(f) = 1 - f^{\frac{2}{3}} \end{cases} \tag{69}$$

Under tensile (axisymmetric) loading, Eq. (68) reduces, as desired, to $\sigma = a\bar{\sigma}$, which is the criterion of Benzerga and Leblond (2014) on account of the identification with Hill's estimate (see Section 5.4). Under pure shear, Eq. (68) reduces to Drucker's estimate, as desired.

On the other hand, Gurson's yield function is:

$$\Phi^{\mathrm{Gur}}(\sigma_{\mathrm{eq}}, \sigma_{\mathrm{m}}; f, \bar{\sigma}) = \frac{\sigma_{\mathrm{eq}}^2}{\bar{\sigma}^2} + 2f\cosh\left(\frac{3}{2}\frac{\sigma_{\mathrm{m}}}{\bar{\sigma}}\right) - 1 - f^2 = 0 \tag{70}$$

Note in passing that Gurson's criterion can be approximated by an elliptic criterion having the form:

$$\Phi^{\mathrm{H}}(\sigma_{\mathrm{eq}}, \sigma_{\mathrm{m}}; f, \bar{\sigma}) = \left(\frac{\sigma_{\mathrm{m}}}{a\bar{\sigma}}\right)^2 + \left(\frac{\sigma_{\mathrm{eq}}}{d\bar{\sigma}}\right)^2 - 1 = 0 \tag{71}$$

which has the virtue of keeping a simpler parallel with Eq. (68) while preserving the Gurson yield points under purely hydrostatic and deviatoric loadings. Here, a is the same as in Eq. $(69)_1$ while $d(f) = 1 - f$.

7.2. Perrin's argument

Perrin (1992) provided a critical analysis of Gurson's heuristic extension to strain hardening, as formulated through Eqs. (67) and (70). Starting from the well-known exact solution giving the yield stress under hydrostatic loading, $\sigma_{\mathrm{m}}^{\mathrm{y}}$, of a hollow sphere made of a rigid–plastic hardenable material, he bounds the latter from *below*:

$$\sigma_{\mathrm{m}}^{\mathrm{y}} > a\langle\bar{\sigma}(\bar{\varepsilon}(\mathbf{x}))\rangle_{V^{\mathrm{m}}} \tag{72}$$

where a is given by Eq. $(69)_1$, $\bar{\sigma}$ is the true flow stress, function of the actual (not fictitious) effective plastic strain in the matrix, $\bar{\varepsilon}$, and V^{m} denotes the volume occupied by the matrix. That hardening is heterogeneous is reflected in the dependence of $\bar{\varepsilon}$ upon location $\mathbf{x}$. Then Perrin bounds from *above* the yield stress under purely deviatoric loading of the same hollow sphere prestrained under hydrostatic pressure:

$$\sigma_{\mathrm{eq}}^{\mathrm{y}} \leq d\langle\bar{\sigma}(\bar{\varepsilon}(\mathbf{x}))\rangle_{V^{\mathrm{m}}} \tag{73}$$

where $d = 1 - f$, as in Eq. (71).

Now, according to Gurson's criterion, Eq. (70), the corresponding yield limits are: $\sigma_{\mathrm{m}}^{\mathrm{y}}|^{\mathrm{Gur}} = a\bar{\sigma}$ and $\sigma_{\mathrm{eq}}^{\mathrm{y}}|^{\mathrm{Gur}} = d\bar{\sigma}$. If these estimates were correct, $\bar{\sigma}$ would be strictly greater than $\langle\bar{\sigma}(\bar{\varepsilon}(\mathbf{x}))\rangle_{V^{\mathrm{m}}}$ by Eq. (72) and smaller or equal to it by Eq. (73), which is impossible.

With this simple, but elegant reasoning, Perrin (1992) shows that the yield stresses under purely deviatoric, $\sigma_{\mathrm{eq}}^{\mathrm{y}}$, and purely spherical, $\sigma_{\mathrm{m}}^{\mathrm{y}}$, loadings are not expressible in terms of a single hardening parameter $\bar{\sigma}$, irrespective of the value taken by the latter; also see Leblond et al. (1995). This pleads in favor of a differential hardening formulation.

A practical implication of the differential hardening effect is the dependence of porosity evolution upon the strain hardening capacity of the matrix material. This dependence is consistent with direct numerical simulations (Koplik and Needleman, 1988) but the Gurson model does not capture it, Fig. 8. This shortcoming is, to be sure, not peculiar to the Gurson model. Any yield criterion of porous material plasticity that takes the form:

$$\Phi(\sigma_{\mathrm{eq}}, \sigma_{\mathrm{m}}; f, \bar{\sigma}) = \hat{\Phi}\left(\hat{\sigma}_{\mathrm{eq}}, \hat{\sigma}_{\mathrm{m}}; f\right); \qquad \hat{\sigma}_{\mathrm{eq}} = \frac{\sigma_{\mathrm{eq}}}{\bar{\sigma}}, \quad \hat{\sigma}_{\mathrm{m}} = \frac{\sigma_{\mathrm{m}}}{\bar{\sigma}} \tag{74}$$

cannot capture the dependence of porosity evolution upon strain hardening.

To best illustrate this, consider axially symmetric proportional stressing such that the triaxiality $T = \sigma_{\mathrm{m}}/\sigma_{\mathrm{eq}}$ is constant and define:

$$\dot{E}_{\mathrm{eq}} = D_{\mathrm{eq}} = \sqrt{\frac{2}{3}\mathbf{D}^{\mathrm{p}\prime} : \mathbf{D}^{\mathrm{p}\prime}}, \quad \text{and} \quad \dot{E}_{\mathrm{m}} = D_{\mathrm{m}} = \frac{1}{3}\,\mathrm{tr}\,\mathbf{D}^{\mathrm{p}} \tag{75}$$

At fixed triaxiality, one has $\hat{\sigma}_{\mathrm{m}} = T\hat{\sigma}_{\mathrm{eq}}$ and, by inverting the yield condition, $\hat{\sigma}_{\mathrm{eq}}$ is entirely determined by T and f:

$$\hat{\Phi}(\hat{\sigma}_{\mathrm{eq}}, T\hat{\sigma}_{\mathrm{eq}}; f) = 0 \tag{76}$$

Now, by integrating Eq. (52) the current porosity is determined by its initial value, f_0, and the current value of E_{m}:

$$f = 1 - (1 - f_0)\exp\left(-3E_{\mathrm{m}}\right) \tag{77}$$

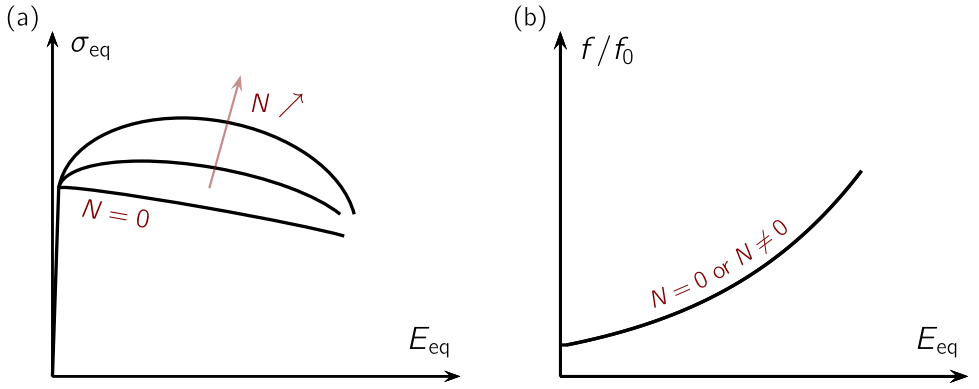

Fig. 8. Effect of strain hardening, as predicted by the Gurson model, using power-law hardening with exponent N: (a) Stress versus strain. (b) Porosity versus strain.

Next, the plastic multiplier $\dot{\gamma}^{\mathrm{H}}$ is eliminated from Eqs. (62) and (64) by considering the ratio

$$\frac{\dot{E}_{\mathrm{m}}}{\dot{E}_{\mathrm{eq}}} = \frac{1}{3}\frac{\partial \boldsymbol{\Phi}/\partial \sigma_{\mathrm{m}}}{\partial \boldsymbol{\Phi}/\partial \sigma_{\mathrm{eq}}} = \frac{1}{3}\frac{\partial \hat{\boldsymbol{\Phi}}/\partial \hat{\sigma}_{\mathrm{m}}}{\partial \hat{\boldsymbol{\Phi}}/\partial \hat{\sigma}_{\mathrm{eq}}} \tag{78}$$

The right-hand side of Eq. (78) is a function of $\hat{\sigma}_{\mathrm{m}}$ and $\hat{\sigma}_{\mathrm{eq}}$: it only depends on the flow stress $\bar{\sigma}$ through those ratios. But at fixed T, $\hat{\sigma}_{\mathrm{m}}$ is set by $\hat{\sigma}_{\mathrm{eq}}$, which only depends on T, f_0 and E_{m}. Thus the porosity versus E_{eq} curve is independent of the flow stress $\bar{\sigma}$ since it is determined by Eq. (77) and the integral curve of Eq. (78); see Fig. 8b.

7.3. Case of unhomogeneous yielding

Whether the heuristic formulation underlying Eqs. (67) and (68) is adequate remains to be investigated. What is paramount is how strain hardening affects unhomogeneous yielding *relative to* homogeneous yielding. A separate analysis for the former is important, but because the two processes are in competition a concurrent analysis is what matters most. Rigorous proofs are out of reach at present because exact solutions are lacking even for simple cases. Yet, some trends may be argued, as developed below.

One key observation is that strain hardening corrections are far more important under shearing states than they are under axisymmetric states of loading. To illustrate this refer to Fig. 9. Admit for the time being that the exact yield stress (thick lines) is greater than the heuristic estimate (thin lines) for a given yielding mode. Under axisymmetric stress states (Fig. 9a) and sufficiently low triaxiality, the unhomogeneous-yield (UY) estimate (solid lines) is sufficiently larger than the homogeneous-yield (HY) estimate (dashed lines) that no hardening correction would change the relative order. In an evolution problem, a transition may eventually occur, aided by porosity-induced softening.

At sufficiently high triaxiality and porosity ($f \geq 0.01$), the UY estimate is lower than the HY estimate (see Fig. 4a in Section 5.4). However, with hardening it is argued that the order of exact values reverses. This reversal holds in the early stages of straining but is bound to revert back to UY becoming dominant again. A rationale is given in Appendix G.

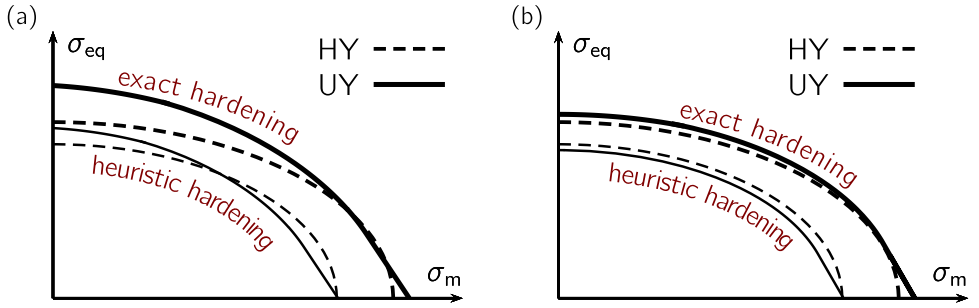

Fig. 9. Effect of hardening on homogeneous (HY) and unhomogeneous yielding (UY) for (a) axisymmetric states of loading ($\Theta = 0$) and (b) shearing states of loading ($\Theta = \pi/6$).

Under shearing states, on the other hand, heuristic estimates and exact values are close to each other so that small corrections can have a major impact on relative ordering (Fig. 9b). Clearly, the heuristic estimates by Eqs. (68) and (71) favor unhomogeneous yielding since $b(f) < d(f)$ for all values of f leading to:

$$\tau^{\mathrm{U,heur}} = (1 - f^{\frac{2}{3}})\bar{\tau} < \tau^{\mathrm{H,heur}} = (1 - f)\bar{\tau} \tag{79}$$

However, the exact values may be re-ordered as:

$$\tau^{\mathrm{U}} > \tau^{\mathrm{H}} \tag{80}$$

at least for the early stages of a loading program. Rationales for the above inequality and a transition back to unhomogeneous yielding are developed in Appendix G.

In spite of the above general bounding properties, it is not clear at present whether a differential hardening formulation is needed for unhomogeneous yielding. An indication may be inferred from analyzing porosity evolution. In any case, what is paramount is that an unhomogeneous yield criterion extended to hardening should satisfy Eq. (80).

Finally, a note on porosity evolution and associated dilation. Regardless of the mode of yielding, plastic dilation decreases with increasing strain hardening. In other words, the more hardenable the matrix the lower the rate of porosity. A rationale for this general trend is that the material hardens more in the vicinity of the hole than away from it. The larger the hardening capacity the harder the layers that surround the pore. This "rigidification" phenomenon is expected to be even stronger under unhomogeneous yielding since the hole is confined between two rigid zones, by the very definition of this mode.

7.4. Differential hardening formulation

There is indication that, at least for relatively large porosity levels ($f \geq 0.01$), a differential hardening formulation is needed. Then the unhomogeneous yield criterion, e.g. as given by Eq. (68), holds as is but with $\bar{\sigma}$ and $\bar{\tau}$ treated as two separate hardening parameters. General expressions for these are yet to be developed. Unlike for homogeneous yielding, the field is in its infancy.

However, as stated above, what matters most is that differential hardening be incorporated for the effective multisurface criterion, which would account for both homogeneous and unhomogeneous yielding. In the proposed extension, the formulation need not be extended to differential hardening for both surfaces; just for the homogeneous-yield surface. Thus, the terms replacing $\bar{\sigma}$ and $\bar{\tau}$ would be related. While this merits study, a general formulation is as follows, illustrated in the isotropic case using the same two surrogate criteria of Eqs. (68) and (70).

For unhomogeneous yielding, the term $\bar{\sigma}$ in Eq. (68) or any criterion of the form $\phi^k(\boldsymbol{\sigma}; \boldsymbol{\alpha}^k, \bar{\sigma}) \leq 0$, is replaced with $\tilde{\sigma}$, an appropriately averaged flow stress over the band occupying volume V_{L}:

$$\tilde{\sigma} = \langle\langle \bar{\sigma} \rangle\rangle_{V_{\mathrm{L}}} \tag{81}$$

where it is understood that $\bar{\sigma}(\bar{\varepsilon}(\mathbf{x}))$ is a function of position and the notation $\langle\langle . \rangle\rangle_{V_{\mathrm{L}}}$ stands for volume averaging with a weight function that favors regions in the vicinity of the void; see Appendix G.

For homogeneous yielding, on the other hand, the term $\bar{\sigma}$, which appears twice in Eq. (70) (likewise in Eq. (71)) is replaced with

$$\begin{cases} \tilde{\sigma} = \langle\langle \bar{\sigma} \rangle\rangle_{V^{\mathrm{m}}} \\ \tilde{\tau} = \langle \bar{\sigma} \rangle_{V^{\mathrm{m}}} \end{cases} \tag{82}$$

the first appearing in the cosh term, the second in the quadratic one. Note that the spatial average involved in defining $\tilde{\tau}$ is the usual one.

A differential hardening formulation based upon the above definitions would satisfy Eq. (80) for reasons developed in Appendix G.

8. Strain-rate hardening

Insofar as unhomogeneous yielding refers to the finite strain concentration within a representative element of porous material, it is applicable to both rate-independent and rate-dependent matrices. The phenomenology differs, however, in an evolution problem. In a rate-independent material, strain concentration in a band is accompanied with elastic unloading outside the band. By way of contrast, the latter region continues to deform in a rate-dependent material, albeit at a rate much lower than inside the band.

To date, the viscoplasticity of porous materials has been analyzed exclusively within confines similar to those of homogeneous yielding, as per the definitions of this paper. For a critical analysis of theoretical approaches see Section 6.5 of the review by Benzerga and Leblond (2010).

Here, strain-rate effects are incorporated in unhomogeneous yielding using the concept of gauge surfaces introduced by Leblond et al. (1994); also see Benzerga and Leblond (2010) for a succinct presentation and subsequent developments. Before doing so, a practical extension of the Gurson model to rate-dependent materials is presented with its main drawback highlighted so as to motivate other developments.

8.1. Heuristic Gurson potential

For practical purposes, an attractive extension of Gurson's model of homogeneous yielding to rate-dependent materials was proposed by Pan et al. (1983). The yield function $\Phi^{\mathrm{Gur}}(\sigma_{\mathrm{eq}}, \sigma_{\mathrm{m}}; f, \bar{\sigma})$ in Eq. (70) is used as a *de facto* plastic potential. The strain-rate direction is then given by:

$$\mathbf{D}^{\mathrm{p}} = \dot{\gamma}^{\mathrm{G}} \frac{\partial \Phi^{\mathrm{Gur}}}{\partial \boldsymbol{\sigma}} \tag{83}$$

The proportionality factor $\dot{\gamma}^{\mathrm{G}}$ is now determined by the heuristic dissipation identity, Eq. (67). The latter no longer serves as an evolution equation for the fictitious ϵ^*, which is specified by a viscoplastic law of the form:

$$\dot{\epsilon}^* = \dot{\epsilon}^*(\epsilon^*, \bar{\sigma}) \tag{84}$$

On the other hand, the matrix flow stress $\bar{\sigma}$ is determined from a consistency condition $\dot{\Phi}^{\mathrm{Gur}} = 0$.

The so-extended Gurson model provides a relatively simple framework for analyzing a range of problems where rate-sensitivity plays a role, e.g. see Benzerga et al. (2016) and references therein. However, the framework suffers from the same drawback as the Gurson model, heuristically extended to strain hardening. It is straightforward to verify from the inherent normality structure that the rate of growth of porosity is still governed by a relation formally similar to Eq. (78). By way of consequence, porosity evolution would be insensitive to strain-rate. For illustration, Fig. 8 would appropriately depict the situation, substituting the hardening exponent N for a rate-hardening exponent. The net stress–strain response would carry the signature of strain-rate sensitivity but the porosity versus strain response would not.

Other variants of the above heuristic extension to rate-dependent materials have been proposed, e.g. Besson (2009). However, they share the same drawback noted above.

8.2. Viscoplastic formulation

Assume a viscoplastic matrix material described by a viscous stress potential of the Norton type with exponent n. Then, its volume average over the porous body defines a macroscopic potential $\Psi(\boldsymbol{\sigma})$ such that:

$$\mathbf{D}^{\mathrm{p}} = \frac{\partial \Psi}{\partial \boldsymbol{\sigma}} \tag{85}$$

The macro-potential Ψ inherits some of the basic properties of its microscopic counterpart, namely it is convex, positively homogeneous of degree $n+1$ in $\boldsymbol{\sigma}$, and satisfies a variational principle such as that embodied in Eq. (15) (Michel and Suquet, 1992).

Because $\Psi(\boldsymbol{\sigma})$ is positively homogeneous of degree $n+1$ there exists a scalar-valued function $\Lambda(\boldsymbol{\sigma})$, positively homogeneous of degree 1, such that:

$$\Psi(\boldsymbol{\sigma}) = \frac{\sigma_0 \dot{\epsilon}_0}{n+1} \left[\frac{\Lambda(\boldsymbol{\sigma})}{\sigma_0} \right]^{n+1} \tag{86}$$

where σ_0 bears the meaning of a yield stress at reference strain rate $\dot{\epsilon}_0$ in the rate-independent limit $n \to \infty$.

Now, introduce a reduced stress as:

$$\hat{\boldsymbol{\sigma}} = \frac{\boldsymbol{\sigma}}{\Lambda} \tag{87}$$

By definition of the so-called gauge factor Λ, the reduced stress $\hat{\boldsymbol{\sigma}}$ is positively homogeneous of degree 0 in $\boldsymbol{\sigma}$. In addition, using the homogeneity property of Ψ one has:

$$\Psi(\hat{\boldsymbol{\sigma}}) = \Psi\left(\frac{1}{\Lambda}\boldsymbol{\sigma}\right) = \left(\frac{1}{\Lambda}\right)^{n+1} \Psi(\boldsymbol{\sigma}) = \frac{\dot{\epsilon}_0}{(n+1)\sigma_0^n} \tag{88}$$

the latter equality resulting from Eq. (86).

The result in Eq. (88) constitutes a basis for introducing the notion of gauge surface for the porous material. Specifically, the gauge surface S is the equipotential surface in the reduced stress space such that $\Psi(\hat{\boldsymbol{\sigma}}) = \dot{\epsilon}_0/((n+1)\sigma_0^n)$ as per Eq. (88). Alternatively, there exists a gauge function $\hat{\Psi}$ such that the gauge surface is defined by:

$$\hat{\boldsymbol{\sigma}} \in S \Leftrightarrow \hat{\Psi}(\hat{\boldsymbol{\sigma}}) = 0 \tag{89}$$

As noted by Leblond et al. (1994) it is easier to obtain an approximation for the gauge function $\hat{\Psi}(\hat{\boldsymbol{\sigma}})$ than for the stress potential $\Psi(\boldsymbol{\sigma})$.

Let $\Phi(\boldsymbol{\sigma})$ denote, as above, the yield function of the porous material in the rate-independent limit. In general, an approximation of the gauge function $\hat{\Psi}(\hat{\boldsymbol{\sigma}})$ is sought whereby the latter (i) is quadratic for $n = 1$ (as required by linearity); and (ii) reduces to $\Phi(\boldsymbol{\sigma})$ for $n \to \infty$.

For homogeneous yielding, an exact solution is available for a hollow sphere under pure pressure. It makes then sense that the approximate $\hat{\Psi}(\hat{\boldsymbol{\sigma}})$ respect such solution. For unhomogeneous yielding, however, not much is known by means of exact solutions in the rate-independent limit, let alone for generally rate-dependent materials. Thus, in general the sought gauge function $\hat{\Psi}(\hat{\boldsymbol{\sigma}})$ should have a structure that obeys criteria (i) and (ii) above.

In general, the choice for $\hat{\Psi}(\hat{\boldsymbol{\sigma}})$ is problem specific. Of interest are, however, unhomogeneous yield criteria that possess the following form[12]:

$$\Phi^{\mathrm{U}}(\sigma,\tau;f,\bar{\sigma}) = \left(\frac{\tau}{\bar{\tau}}\right)^2 + 2f_b\cosh\left(\frac{\sigma}{\bar{\sigma}}\right) - 1 - f_b^2 = 0 \tag{90}$$

The limit stresses in shear and pressure are respectively: $(1-f_b)\bar{\tau}$ and $-\bar{\sigma}\ln f_b$, the same as those given by Eq. (68).

With Eq. (90) as the rate-independent reference, a suitable choice for the gauge function would be:

$$\hat{\Psi}^{\mathrm{U}}(\hat{\sigma},\hat{\tau};f) = \hat{\tau}^2 + f_b\left[H_n(\hat{\sigma}) + \frac{n-1}{n+1}\frac{1}{H_n(\hat{\sigma})}\right] - 1 - \frac{n-1}{n+1}f_b^2 \tag{91}$$

where

$$\hat{\tau} = \frac{\tau}{\Lambda}; \qquad \hat{\sigma} = \frac{\sigma}{\Lambda} \tag{92}$$

$$H_n(\hat{\sigma}) = \left[1 + \frac{1}{n}|\hat{\sigma}|^{\frac{n+1}{n}}\right]^n \tag{93}$$

To account for strain-hardening, Eq. (86) is rewritten as:

$$\Psi(\sigma,\tau;f,\bar{\sigma}) = \frac{\bar{\sigma}\dot{\epsilon}_0}{n+1}\left[\frac{\Lambda(\sigma,\tau;f)}{\bar{\sigma}}\right]^{n+1} \tag{94}$$

where $\bar{\sigma}$ is the current flow stress, formulated either using the heuristic extension (Section 7.1) or the differential hardening format in Section 7.4.

The viscous potential Ψ is determined once the gauge factor Λ has been specified. The latter is determined implicitly from the gauge condition, Eq. (91). In the rate-independent limit ($n\to\infty$), it follows from Eq. (85) and Eq. (94) that $\mathbf{D}^{\mathrm{p}}$ is zero if $\Lambda<\bar{\sigma}$ and infinite if $\Lambda>\bar{\sigma}$; thus the yield condition is $\Lambda=\bar{\sigma}$. It follows that if plastic flow does occur, Eq. (89) now reads $\hat{\Psi}(\boldsymbol{\sigma}/\bar{\sigma})=0$. Hence, up to some unimportant scaling factor $\bar{\sigma}$, S is nothing but the yield surface, and $\hat{\Psi}$ is nothing but the yield function. Furthermore, the so-introduced function H_n has the desired property that $H_n(\hat{\sigma})\to\exp(\hat{\sigma})$ when $n\to\infty$ such that Eq. (90) is indeed recovered.

The extension of the elliptic criterion is more straightforward, as the following gauge function would meet above criteria (i) and (ii):

$$\hat{\Psi}^{\mathrm{U}}(\hat{\sigma},\hat{\tau};f) = \left[\left(\frac{\sigma}{a\bar{\sigma}}\right)^2 + \left(\frac{\tau}{b\bar{\tau}}\right)^2\right]^{\frac{n+1}{2}} - 1 \tag{95}$$

Clearly, an elliptic yield function or a yield function of the type of Eq. (90) are amenable to the above extensions. How the procedure may be generalized to other unhomogeneous yield criteria merits study.

9. Thermodynamic consistency

We briefly consider thermodynamic restrictions to the purely mechanical theory considered thus far within the framework of generalized standard materials (Halphen and Son, 1975). Furthermore, we shall restrict the presentation to infinitesimal transformations and rate-independent behavior.

The constitutive relation of a generalized standard material is specified through two thermodynamic potentials, the (Helmholtz) specific free energy ψ and the dissipation $\mathcal{D}$. The state of the material is defined by the total strain $\boldsymbol{\epsilon}$ and a collection $\mathbf{a}$ of internal state variables. The free energy $\psi(\boldsymbol{\epsilon},\mathbf{a})$ must be convex with respect to the variables $\boldsymbol{\epsilon}$, $\mathbf{a}$ taken *separately*. The dissipation potential $\mathcal{D}(\dot{\mathbf{a}})$ must be convex and positive with $\mathcal{D}(\dot{\mathbf{a}})=0$ only if $\dot{\mathbf{a}}=\mathbf{0}$.

The free energy potential provides the stress tensor $\boldsymbol{\sigma}$ and thermodynamic forces $\mathbf{A}$ associated with $\mathbf{a}$:

$$\boldsymbol{\sigma} = \frac{\partial\psi}{\partial\boldsymbol{\epsilon}} \quad \text{and} \quad \mathbf{A} = -\frac{\partial\psi}{\partial\mathbf{a}} \tag{96}$$

The dissipation potential governs the evolution of internal variables through:

$$\mathbf{A}\in\partial\mathcal{D}(\dot{\mathbf{a}}) \Leftrightarrow \dot{\mathbf{a}}\in\partial\tilde{\mathcal{D}}(\mathbf{A}) \tag{97}$$

where the $\tilde{(\cdot)}$ denotes the Legendre–Fenchel transform and $\partial f(\mathbf{x})$ is the subdifferential of the continuous (not necessarily differentiable) function f at $\mathbf{x}$.

For rate-independent behavior, $\mathcal{D}$ is positively homogeneous of degree 1. Thus, $\tilde{\mathcal{D}}(\mathbf{A})$ is the index function of a closed convex set $\bar{C}$ in the space of thermodynamic forces. This set gives the domain of reversibility and is defined by an inequality of the type: $\bar{\Phi}(\mathbf{A})\le 0$. Thus, the set of subgradients $\partial\tilde{\mathcal{D}}(\mathbf{A})$ reduces to $\{\mathbf{0}\}$ if $\mathbf{A}\in\bar{C}$, to the semiline $\{\eta\frac{\partial\bar{\Phi}}{\partial\mathbf{A}},\eta\ge 0\}$ if $\mathbf{A}\in\partial\bar{C}$, the latter denoting the boundary of $\bar{C}$, and to the empty set if $\mathbf{A}\notin\bar{C}$. As a result, the evolution equation of the internal variables obeys a generalized normality rule:

$$\dot{\mathbf{a}} = \eta\frac{\partial\bar{\Phi}}{\partial\mathbf{A}}, \qquad \eta = \begin{cases} =0 & \text{if} \quad \bar{\Phi}(\mathbf{A})<0 \\ \ge 0 & \text{if} \quad \bar{\Phi}(\mathbf{A})=0 \end{cases} \tag{98}$$

[12] A criterion developed by Keralavarma and Chockalingam (2016) is of this form, but involves complex expressions, which are here simplified on account of the identification with Hill's solution; see Section 5.4.

This is equivalent to Eq. (97)$_2$ and guarantees non-negative dissipation among other properties.

Most porous material plasticity models derived by homogenization (see Section 3.1) assume a matrix material that obeys an associated J_2 flow theory. This holds irrespective of whether the resulting structure of constitutive relations pertains to homogeneous or unhomogeneous yield type models. That a J_2 matrix is a generalized standard material has long been established. Had the same character been guaranteed by mere homogenization one would have been able to show *a priori* the thermodynamic consistency of porous material plasticity models, *all at once*. That such an immensely useful result is impossible to obtain *a priori* is rooted in the challenging problem of "homogenizing" the free energy part of the constitution. An indirect manifestation[13] of this difficulty was encountered in considering strain hardening formulations, see Section 7.

It appears, therefore, that the issue of thermodynamic consistency of the resulting constitutive relations is important, especially considering the fact that heuristic extensions are often proposed before applications. Enakoutsa et al. (2007) addressed the issue for a class of homogeneous yield models.

Here, we seek to study the generalized standard material character of a relatively simple subclass of unhomogeneous yield models. We consider isotropic models with the heuristic extension to hardening of Section 7. The overall yield criterion is supposed to be given through a function $\Phi^{\mathrm{U}}(\boldsymbol{\sigma}, \bar{\sigma}, f_b)$, convex with respect to $\boldsymbol{\sigma}$, where it is emphasized that all stress dependence enters through the normal and shear tractions acting on some optimal band, and f_b is the band porosity while f is the total porosity. An associated flow rule is assumed and the evolution of the strain hardening parameter ϵ^* is rewritten from Eq. (67):

$$(c - f)\bar{\sigma}(\epsilon^*)\dot{\epsilon}^* = \boldsymbol{\sigma} : \dot{\boldsymbol{\varepsilon}}^{\mathrm{p}} \tag{99}$$

Recall that $c = f/f_b$ is the band volume fraction.

Drawing upon the procedure of Enakoutsa et al. (2007), the internal state of the material is supposed to be given by prescribing[14] the plastic strain, $\boldsymbol{\varepsilon}^{\mathrm{p}}$, the strain hardening parameter, ϵ^*, as well as f and c. Define a free energy potential given by:

$$\psi(\boldsymbol{\varepsilon}, \boldsymbol{\varepsilon}^{\mathrm{p}}, \epsilon^*, f, c) = \frac{1}{2}(\boldsymbol{\varepsilon} - \boldsymbol{\varepsilon}^{\mathrm{p}}) : \mathbb{C}^{-1} : (\boldsymbol{\varepsilon} - \boldsymbol{\varepsilon}^{\mathrm{p}}) + \beta \int_0^{\epsilon^*} \bar{\sigma}(\epsilon)\, \mathrm{d}\epsilon + \bar{\psi}(f, c) \tag{100}$$

where, as in Section 6.2, $\mathbb{C}$ denotes the fourth-order elastic compliance tensor and $\bar{\sigma}(\epsilon)$ represents the uniaxial stress–strain response. Also, $\beta > 0$ and $\bar{\psi}(f, c)$ respectively denote a constant and a strictly convex function to be eventually determined.

The quadratic form defined by $\mathbb{C}$ being positive-definite, the above free energy is strictly convex with respect to the total strain. For the same reason, ψ is strictly convex with respect to the plastic strain. The second term in Eq. (100) is a strictly convex function of ϵ^* since only positive hardening is considered. Being the sum of three strictly convex functions, ψ is thus (strictly) convex in the global variable $(\boldsymbol{\varepsilon}^{\mathrm{p}}, \epsilon^*, f, c)$, as required.

The thermodynamic forces associated with the internal variables of ψ are obtained by specializing Eq. (96)$_2$:

$$\begin{cases} \mathbf{A}^{\boldsymbol{\varepsilon}^{\mathrm{p}}} = -\dfrac{\partial \psi}{\partial \boldsymbol{\varepsilon}^{\mathrm{p}}} = \mathbb{C}^{-1} : (\boldsymbol{\varepsilon} - \boldsymbol{\varepsilon}^{\mathrm{p}}) = \boldsymbol{\sigma} \\ A^{\epsilon^*} = -\dfrac{\partial \psi}{\partial \epsilon^*} = -\beta \bar{\sigma} \end{cases} \qquad \begin{cases} A^f = -\dfrac{\partial \psi}{\partial f} = -\dfrac{\partial \bar{\psi}}{\partial f} \\ A^c = -\dfrac{\partial \psi}{\partial c} = -\dfrac{\partial \bar{\psi}}{\partial c} \end{cases} \tag{101}$$

Next, one needs to show that the dissipation potential is convex with respect to its arguments or, equivalently, that the reversibility domain $\bar{C}$ is convex. To this end, it suffices to show that the yield function, expressed in the space of thermodynamic forces is convex. Had the mapping between the variables $(\boldsymbol{\sigma}, \bar{\sigma}, f_b)$ and the thermodynamic forces $(\mathbf{A}^{\boldsymbol{\varepsilon}^{\mathrm{p}}}, A^{\epsilon^*}, A^f, A^c)$ been linear and had the yield function $\Phi^{\mathrm{U}}(\boldsymbol{\sigma}, \bar{\sigma}, f_b)$ been convex, the convexity of domain $\bar{C}$ would have followed. However, the former is not evident (unless some very special choice is made of $\bar{\psi}$) and the latter is not true, for the function Φ^{U} is convex with respect to the stress $\boldsymbol{\sigma}$ but not with respect to the other two variables. To lift this difficulty, therefore, we shall prescribe that the void volume and band volume fractions be considered as *fixed*: they are no longer treated as internal variables.[15] This amounts to taking $\bar{\psi} = 0$ in Eq. (100). The convexity of $\bar{C}$ then hinges on the convexity of the function $\hat{\Phi}^{\mathrm{U}}(\hat{\boldsymbol{\sigma}}; f_b) = \Phi^{\mathrm{U}}(\boldsymbol{\sigma}, \bar{\sigma}, f_b)$ where $\hat{\boldsymbol{\sigma}} = \boldsymbol{\sigma}/\bar{\sigma}$; see Appendix I for a proof.

Last, the evolution of internal variables must be governed by generalized normality, Eq. (98) which, using Eq. (101), is specialized to:

$$\begin{cases} \dot{\boldsymbol{\varepsilon}}^{\mathrm{p}} = \eta \dfrac{\partial \bar{\Phi}}{\partial \mathbf{A}^{\boldsymbol{\varepsilon}^{\mathrm{p}}}} = \eta \dfrac{\partial \Phi}{\partial \boldsymbol{\sigma}} \\ \dot{\epsilon}^* = \eta \dfrac{\partial \bar{\Phi}}{\partial A^{\epsilon^*}} = -\dfrac{\eta}{\beta} \dfrac{\partial \Phi}{\partial \bar{\sigma}} \end{cases} \tag{102}$$

[13] Perhaps a better illustration of the challenge is encountered in dislocation plasticity (Benzerga et al., 2005). The microscale free energy may be a simple quadratic function of the microscopic strain, the latter being purely elastic since dislocation-mediated plasticity is confined to planes (or surfaces in wavy slip under finite deformations). The macroscale free energy may be written as the sum of a quadratic term in some volume-averaged macroscopic elastic strain and a term that strictly depends on current dislocation positions. Obtaining an analytical expression of the macroscopic free energy from the microscopic one is still an open question.

[14] Physically, the internal state of a plastically deformed body is defined by the current positions of defects, say dislocations in crystals, not the plastic strain. But this prescription, common in the literature, is accepted here.

[15] This, of course, would have consequences in terms of the usual properties sought under a generalized standard material description, e.g. regarding existence and uniqueness of solutions.

The first of these is verified as it corresponds to standard normality, which generally holds in porous material plasticity; see Section 4.2. On the other hand, Eq. $(102)_2$ only holds if a suitable choice is made of constant β. To see this, operate the same change of variable as above, namely $\hat{\boldsymbol{\sigma}} = \boldsymbol{\sigma}/\bar{\sigma}$ to obtain:

$$\frac{\partial \boldsymbol{\Phi}}{\partial \bar{\sigma}} = \frac{\partial \hat{\boldsymbol{\Phi}}}{\partial \hat{\boldsymbol{\sigma}}} : \frac{\partial \hat{\boldsymbol{\sigma}}}{\partial \bar{\sigma}} = -\frac{1}{\bar{\sigma}^2}\boldsymbol{\sigma} : \frac{\partial \hat{\boldsymbol{\Phi}}}{\partial \hat{\boldsymbol{\sigma}}} \tag{103}$$

Then, expressing Eq. $(102)_1$ in terms of $\hat{\boldsymbol{\Phi}}$:

$$\dot{\boldsymbol{\epsilon}}^{\mathrm{p}} = \frac{\eta}{\bar{\sigma}}\frac{\partial \hat{\boldsymbol{\Phi}}}{\partial \hat{\boldsymbol{\sigma}}} \tag{104}$$

so that

$$\frac{\partial \boldsymbol{\Phi}}{\partial \bar{\sigma}} = -\frac{1}{\eta \bar{\sigma}}\boldsymbol{\sigma} : \dot{\boldsymbol{\epsilon}}^{\mathrm{p}} \tag{105}$$

It follows that Eq. $(102)_2$ would hold only if

$$\dot{\epsilon}^{*} = \frac{1}{\beta \bar{\sigma}}\boldsymbol{\sigma} : \dot{\boldsymbol{\epsilon}}^{\mathrm{p}} \tag{106}$$

Given Eq. (99), Eq. $(102)_2$ would hold only if

$$\beta = c - f \tag{107}$$

This is possible once f and c are not treated as internal state variables, consistent with the findings of Enakoutsa et al. (2007) for the Gurson model extended to hardening.

The above illustrates the generalized standard material character of a subclass of unhomogeneous yield models extended heuristically to strain hardening. Clearly, more work is needed on the thermodynamic consistency of other formulations.

10. Length scale effect

It remains to understand why a strain derived from Eqs. (7) and (8), which is *nonuniform* inside the elementary volume, does not lead to a gradient-type formulation. In other words, the question we close with is this: why does the theory of unhomogeneous yielding presented herein lack a length scale?

It is edifying to reason in one dimension first. After all, an integrity basis of unhomogeneous deformation consists of the two fundamental modes depicted in Fig. 2. Consider a velocity profile for the opening mode of unhomogeneous yielding, assuming that the centroid (taken as the origin) is fixed, Fig. 10. The axial velocity on the (lateral) boundary must be constant in the rigid zones while changing sign between the top and bottom. Inside the band, the velocity profile is linear, as per a simplified version of Eq. (7). In order to render explicitly the inherent gradient, one needs to approximate the step-wise velocity with some C^1 function (shown as a thin line in the figure). A judicious choice would be of the form:

$$v_n(x) = \bar{a}x + \frac{1}{2}\operatorname{sgn} x\, \bar{b}x^2 \tag{108}$$

with $\bar{a}$, $\bar{b}$ constants and $x = \mathbf{n}\cdot\mathbf{x}$ a position variable normal to the band. It follows immediately that the average strain-rate

$$\langle \dot{\epsilon} \rangle = \frac{1}{H}\int_{-H/2}^{H/2} v_n'(x)\,\mathrm{d}x = \bar{a} \tag{109}$$

is independent of the coefficient of the higher order term, $\bar{b}$. Here, $\dot{\epsilon}$ refers to the local strain-rate. Likewise for the sliding mode, taking a transverse velocity $v_m(x) = \mathbf{v}\cdot\mathbf{m}$ as a function of $x = \mathbf{n}\cdot\mathbf{x}$ of the same type as above would lead to $\langle \dot{\gamma} \rangle = \bar{a}$ where $\dot{\gamma}$ refers to the local shear rate.

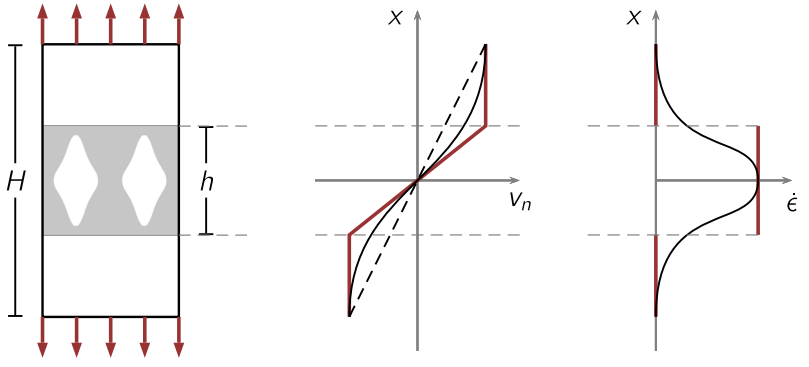

Fig. 10. Boundary velocity and strain-rate profiles for the opening mode.

Generalizing to three dimensions, a nonuniform boundary velocity could be viewed as an expansion to some order in the position vector $\mathbf{x}$. A linear boundary velocity leads to a uniform and gradient-free macroscopic strain. The simplest extension would take the form (Gologanu et al., 1997):

$$\forall \mathbf{x} \in \partial V, \quad \mathbf{v}(\mathbf{x}) = \mathbf{A}\mathbf{x} + \frac{1}{2}\mathbf{B}(\mathbf{x} \otimes \mathbf{x}) \tag{110}$$

where $\mathbf{A}$ and $\mathbf{B}$ are constant tensors of second and third rank, respectively. Minimal constraints on these are that $\mathbf{A}$ be symmetric and $\mathbf{B}$ symmetric in its *second* and *third* indices. It may be shown that (see Appendix H)

$$\langle d_{ij}(\mathbf{x})\rangle_{V(\mathbf{X})} = A_{ij} + \frac{1}{2}(B_{ijk} + B_{jik})X_k \tag{111}$$

where

$$X_k = \frac{1}{V}\int_V x_k \, \mathrm{d}V \tag{112}$$

denotes the position of the centroid of elementary cell V, hence the notation $V(\mathbf{X})$ to emphasize the dependence upon $\mathbf{X}$. Thus, a nonuniform boundary velocity is bound to deliver an average strain-rate that depends on moments of the position vector (here the first moment only). As such, the average strain rate in Eq. (111) may be rewritten so as to exhibit a gradient:

$$\mathbf{D} \equiv \langle \mathbf{d}(\mathbf{x})\rangle \quad \Rightarrow \quad D_{ij;k}(\mathbf{X}) = \frac{1}{2}(B_{ijk} + B_{jik}) \tag{113}$$

where

$$(\cdot)_{;k} \equiv \frac{\partial}{\partial X_k}$$

With the above in mind, it becomes clear that not all non-uniform boundary velocities complying with the format of Eq. (110) lead to a macroscopic strain-rate gradient. A subset of those, characterized with a tensor $\mathbf{B}$ that is *antisymmetric* in its *first* and *second* indices, would be gradient-free.

Obviously, the step-wise boundary velocity defined by Eqs. (7) and (8) does not fit the format of Eq. (110). The point being made is that a C^1 approximation of it would meet the format of Eq. (110), as illustrated in the one-dimensional example above, while having a $\mathbf{B}$ that meets the above additional constraint $B_{ijk} = -B_{jik}$. It is then understood how both the velocity defined by Eqs. (7) and (8) and its C^1 approximation can be gradient-free. That the latter is true has been established for an arbitrary $\mathbf{B}$ meeting the stated condition. That the velocity in Eqs. (7) and (8) delivers a gradient-free overall strain may be made explicit by evaluating the average strain-rate:

$$\langle \mathbf{d}\rangle = c\mathbf{L} + (1-c)\mathbf{U} = \mathbf{U} + \frac{c}{h}\mathbf{v}_0 \otimes^{\mathrm{s}} \mathbf{n} \tag{114}$$

or in indicial notation

$$\langle d_{ij}\rangle = U_{ij} + D_{kk}n_in_j + n_kD_{kl}m_l(m_in_j + m_jn_i) \tag{115}$$

where use has been made of Eq. (9) then Eq. (10).

The absence of a length scale in the theory does not mean that a length scale cannot be incorporated. On the contrary, the theory identifies rather clearly two length scales at which strain gradients may play an important role.[16] The most important strain gradient is across the band. If the thickness of the latter is limited by the void size, as is likely in most evolution problems, then the plastic theory used in the band must be applicable. This implies a minimum void size below which a continuum theory would cease to be valid. The other gradient occurs within the band and manifests mostly in the context of hardening effects. That gradient involves the void spacing within the band.

11. Summary

Below is a recollection of key results:

1. Boundary conditions that accommodate finite strain concentration in a band are formulated. For space-filling cells, those are a subset of periodic boundary conditions. Otherwise, the boundary conditions apply to any type of geometry. Unlike general periodic conditions, they satisfy the Hill–Mandel lemma irrespective of resolution. A practically useful case is when plastic stretch is only possible normal to the band. That is unhomogeneous yielding.
2. There are only two possible fundamental modes of unhomogeneous yielding: opening and sliding. Both are pore-mediated but porosity is only necessary for opening. In general, a reduced dissipation function may thus be solely written in terms of two kinematic parameters.
3. If macro-unhomogeneous deformation is considered, then a universal structure of constitutive relations emerges with $\Pi(\dot{\epsilon}, \dot{\gamma})$, $\phi(\sigma, \tau)$, etc. The unhomogeneous yield criterion of a porous material depends, in intrinsic form, on the resolved normal and shear stresses. Various formats may thus be explored *a posteriori* to illustrate key trends.

[16] This is unlike most gradient theories of plasticity, which because of their phenomenological character, posit a length scale simply out of mathematical consistency with no *a priori* physical meaning.

4. The exact criterion for unhomogeneous yielding must lie between a piecewise-constant ($\max\{|\sigma|, |\tau|\}$ type) criterion and a linear criterion. For specific geometries, the exact yield surface is known to be close to an elliptic criterion while being exterior to it.
5. Specializing the theory to isotropic behavior reveals the following:
   (a) Unhomogeneous yielding is possible in one of two competing modes: (i) normal yielding, which corresponds to opening normal to a principal stress direction; or (ii) yielding under combined tension and shear (concurrent opening and sliding) in a principal plane. This encompasses shear yielding with sliding only.
   (b) The exact yield criterion must lie between the two extremes of Rankine–Tresca and Mohr–Coulomb criteria, both of which exhibit unphysical singularities.
   (c) When yielding is by combined tension and shear, the orientation of the yield system is fully determined by the format of the intrinsic criterion. In engineering practice, that may readily provide the orientation of the failure plane. In particular, whether the orientation depends on the stress ratios or stress magnitudes can be determined *a priori*.
   (d) The Mohr–Coulomb criterion does not predict normal yielding while all other criteria do.
   (e) Unhomogeneous yielding manifests as a competition between a maximum shear stress criterion, at low amounts of pressure, and a maximum normal stress criterion at high amounts of pressure.
   (f) The Rankine–Tresca criterion typifies key attributes of unhomogeneous yielding in the Haigh–Westergaard space. The octahedral section is a hexagon at low pressures, a triangle at high pressures and an evolving nonagon at intermediate pressures. The exact yield surface would have rounded regions near axisymmetric states dependent on the intrinsic yield curve.
   (g) A universal feature among all criteria of unhomogeneous yielding is the presence of a corner, hinting at a physically meaningful region of extreme curvature on the hydrostatic axis. The practical implications of this are paramount for moderate to high porosity levels, and possibly for all porosity levels, because of this: Hill's classical exact yield pressure of the hollow sphere may never be the true exact solution when tested against the possibility of unhomogeneous yielding in an aggregate. Elucidating this warrants, however, sustained research efforts.
   (h) For small to vanishing strain-hardening capacity of the matrix, the entire meridional section of the yield locus is dominated by unhomogeneous yielding for shearing states.
6. The general theory of unhomogeneous yielding accounts for a finite number of yield systems with the following characteristics:
   (a) It is a multisurface theory, just like crystal plasticity but with additional dependence upon the resolved normal stress.
   (b) Each surface evolves due to hardening and porosity-related internal parameters. The overall structure of the evolution equations is completely set by the kinematic constraints that define unhomogeneous yielding as well as plastic incompressibility of the parent material.
7. Strain hardening plays a key role in determining the yielding mode. In particular, for shearing states conventional heuristic extensions would fail to predict proper behavior in an evolution problem. Whether a differential hardening formulation is needed remains unsettled and is problem-dependent. Regardless, unhomogeneous yield criteria should be sought where the effective yield strength is the average of the matrix flow stress itself, not an estimate of it for the average effective strain.
8. Accounting for strain-rate hardening is relatively straightforward using the concept of gauge surface. Unlike an approach that employs the yield function as a plastic potential, this approach not only reproduces the rate-sensitivity of the overall flow stress of the porous material but also of porosity evolution.
9. Thermodynamic consistency of a subclass of unhomogeneous yield models was analyzed within the framework of generalized standard materials. The preliminary analysis implies *a priori* restrictions on algorithms for integrating the nonlinear constitutive relations. For a purely mechanical theory, the most important restriction is that porosity attributes, at least within an eulerian description, must be integrated explicitly.
10. No length scale is inherent to the theory of unhomogeneous yielding developed here. The nonuniform boundary conditions introduced are free of any strain gradients. A gradient formulation may be developed, at the expense of simplicity, which would have to proceed from a C^1 generalization of the boundary conditions introduced herein.
11. Open questions remain on nearly every aspect summarized above. What is of particular importance is to apply a complete set of constitutive relations to problems that have either not been addressed heretofore or tackled with *ad hoc* formulations. Not only are such problems encountered in ductile failure but more broadly in the mechanics of porous materials.

Declaration of competing interest

The authors declare that they have no known competing financial interests or personal relationships that could have appeared to influence the work reported in this paper.

Data availability

Data will be made available on request

Acknowledgments

The author acknowledges financial support from the U.S. Fulbright Scholar Program during his sabbatical at Ecole Nationale Polytechnique in Algiers in 2022. He is also grateful to the National Science Foundation, United States of America (grant CMMI-1932975) and the Lawrence Livermore National Laboratory, United States of America (master agreements B599687 and B602391) for funding research that is synergistic with this work.

Appendix A. Proof of Eq. (2)

An original proof of this known result[17] is given here. Start from the left-hand side of Eq. (2). Add to it and subtract from it the second term. There are now three occurrences of the same term, $\boldsymbol{\Sigma} : \mathbf{D} = \langle \sigma_{ij} \rangle \langle v_{i,j} \rangle$ where the kinematic relations and symmetry of $\boldsymbol{\sigma}$ have been used. Rewrite each occurrence in a different way:

$$\begin{aligned} \langle \sigma_{ij}\, d_{ij} \rangle - \Sigma_{ij}\, D_{ij} + \Sigma_{ij}\, D_{ij} - \Sigma_{ij}\, D_{ij} &= \frac{1}{V} \int_V \sigma_{ij} d_{ij}\, \mathrm{d}V \\ - \langle \sigma_{ij} \rangle \frac{1}{V} \int_{\partial V} v_i n_j\, \mathrm{d}S + \langle \sigma_{ij} \rangle \langle v_{i,j} \rangle &- \frac{1}{V} \int_{\partial V} t_i x_j\, \mathrm{d}S\ \langle v_{i,j} \rangle \end{aligned} \tag{A.1}$$

The divergence theorem was used in the first occurrence and equilibrium in the third. Thus,

$$\langle \sigma_{ij}\, d_{ij} \rangle - \Sigma_{ij}\, D_{ij} = \frac{1}{V} \int_{\partial V} t_i v_i\, \mathrm{d}S - \langle \sigma_{ij} \rangle \frac{1}{V} \int_{\partial V} v_i n_j\, \mathrm{d}S + \delta_{ij} \langle \sigma_{jk} \rangle \langle v_{k,i} \rangle - \frac{1}{V} \int_{\partial V} t_k x_i\, \mathrm{d}S\ \langle v_{k,i} \rangle \tag{A.2}$$

where the principle of virtual power was used for the first term on the right-hand side. Also, the identity tensor was introduced in the third term so as to write the inner product as the trace of a tensor product. Finally, dummy indices were simply rearranged in the fourth term. All but the third term are now surface integrals. This is fixed by using the identity (true by virtue of the divergence theorem):

$$\delta_{ij} = \frac{1}{V} \int_{\partial V} x_i n_j\, \mathrm{d}S \tag{A.3}$$

Combining all integrals gives:

$$\langle \sigma_{ij}\, d_{ij} \rangle - \Sigma_{ij}\, D_{ij} = \frac{1}{V} \int_{\partial V} \left[t_i v_i - \langle \sigma_{ij} \rangle v_i n_j + x_i n_j \langle \sigma_{jk} \rangle \langle v_{k,i} \rangle - t_k x_i \langle v_{k,i} \rangle \right] \mathrm{d}S \tag{A.4}$$

Note that $\langle \cdot \rangle$ terms are constants that go in and out of integrals at will. Now, grouping terms in two integrand pairs yields:

$$\langle \sigma_{ij}\, d_{ij} \rangle - \Sigma_{ij}\, D_{ij} = \frac{1}{V} \int_{\partial V} \left[v_i (t_i - \langle \sigma_{ij} \rangle n_j) + x_i \langle v_{k,i} \rangle (n_j \langle \sigma_{jk} \rangle - t_k) \right] \mathrm{d}S \tag{A.5}$$

Swapping dummy indices i and k in the second grouping enables factorization as:

$$\langle \sigma_{ij}\, d_{ij} \rangle - \Sigma_{ij}\, D_{ij} = \frac{1}{V} \int_{\partial V} \left[t_i - \langle \sigma_{ij} \rangle n_j \right] \left(v_i - x_k \langle v_{i,k} \rangle \right) \mathrm{d}S \tag{A.6}$$

which provides the desired result in Eq. (2) upon substituting for $t_i = \sigma_{ij} n_j$.

Appendix B. Proof of Eq. (9)

First, it is shown that tensors $\mathbf{L}$ and $\mathbf{U}$ introduced in Eqs. (7) and (8) are the average rates of deformation in V_{L} (inside the band) and V_{U} (outside), respectively:

$$\langle \mathbf{d} \rangle_{V_{\mathrm{L}}} = \mathbf{L}, \qquad \langle \mathbf{d} \rangle_{V_{\mathrm{U}}} = \mathbf{U} \tag{B.1}$$

This is not as straightforward as when the entire volume is uniformly constrained. Eq. $(B.1)_1$ holds irrespective of the choice made for $\bar{\boldsymbol{\Omega}}$ in Eq. (7) and follows from the anti-symmetry of $\bar{\boldsymbol{\Omega}}$. On the other hand, Eq. $(B.1)_2$ is only valid because $\mathbf{v}_0$ is made constant thanks to a specific choice of $\bar{\boldsymbol{\Omega}}$, to be elucidated further below.

With reference to Fig. 1, strain-rate compatibility imposes that the in-plane components must be the same:

$$L_{\alpha\alpha} = U_{\alpha\alpha} = D_{\alpha\alpha} \qquad \alpha \neq n \tag{B.2}$$

This alone shows that the difference in strain-rate must be of the form:

$$\mathbf{L} - \mathbf{U} = \mathbf{q} \otimes^{\mathrm{s}} \mathbf{n} \tag{B.3}$$

[17] Nemat-Nasser and Hori (1993) attribute the result to three sources: Hill (1967) cited in the main text, another paper of Hill's from 1963 and a paper by Mandel in 1980. Hill's two papers do not contain Eq. (2), let alone the general proof. Mandel's paper is inaccessible (incidentally, Nemat-Nasser and Hori, 1993 have a wrong citation to it.) Yet, the result must have been known to both Hill and Mandel. Also, the proof in Nemat-Nasser and Hori (1993) uses direct notation and works its way backward from the result, i.e. the right-hand side of Eq. (2).

with $\mathbf{q} = \alpha\mathbf{m} + \beta\mathbf{n}$ an arbitrary vector that can be decomposed as written using the band normal $\mathbf{n}$ and an arbitrary (for now) unit vector $\mathbf{m}$ in the plane of the band. On the other hand, the normal components are related through the standard relation:

$$\mathbf{n}\cdot\mathbf{D}\mathbf{n} \equiv D_{nn} = cL_{nn} + (1-c)U_{nn} \qquad \text{no sum on } n \tag{B.4}$$

where c denotes the band volume fraction. Since, by definition, all dilation is confined to the band, plastic incompressibility outside of it is expressed as (neglecting elasticity for now):

$$\mathrm{tr}\,\mathbf{U} = U_{nn} + 2U_{\alpha\alpha} = 0 \tag{B.5}$$

Substituting this result in Eq. (B.4) gives, on account of Eq. (B.2):

$$L_{nn} = D_{nn} + \frac{1-c}{c}D_{kk} \qquad \text{sum on } k \tag{B.6}$$

Thus, the diagonal components of $\mathbf{L}$ and $\mathbf{U}$ are entirely set by those of the overall rate of deformation $\mathbf{D}$. For convenience, they are recollected here (no sum on either α or n):

$$\begin{cases} U_{\alpha\alpha} = D_{\alpha\alpha} & \alpha \neq n \\ U_{nn} = -2D_{\alpha\alpha} \end{cases} \qquad \begin{cases} L_{\alpha\alpha} = D_{\alpha\alpha} & \alpha \neq n \\ L_{nn} = \dfrac{1}{c}D_{nn} + 2\dfrac{1-c}{c}D_{\alpha\alpha} \end{cases} \tag{B.7}$$

The shear components, however, cannot be solely determined from the kinematical constraints. To fix ideas, if $\mathbf{m}$ denotes a unit vector in the direction of resolved shear rate D_{nm}, assuming no shearing outside the band (i.e. $U_{nm} = 0$) leads to

$$L_{nm} = \frac{1}{c}D_{nm} \tag{B.8}$$

This would be the case in the absence of strain-hardening as the regions outside the band would move as quasi-rigid blocks. In general, to account for shearing outside the band, one may write: $L_{nm} = C\,D_{nm}/c$, where $1/2 \leq C \leq 1$, dependent on the constitutive response.

It follows then from Eqs. (B.7) and (B.8) that the vector $\mathbf{q}$ in Eq. (B.3) is entirely set by the overall rate of deformation following:

$$\mathbf{q} = \frac{D_{kk}}{2c}\mathbf{n} + \frac{D_{nm}}{c}\mathbf{m} \tag{B.9}$$

where the factor $1/2$ results from considering a symmetric dyad in Eq. (B.3). The above equation specifies coefficients α and β introduced after Eq. (B.3); they will be used below as a shorthand notation.

Together, Eqs. (B.3) and (B.9) establish the result inferred from combining Eqs. (9) and (10). It remains to relate $\mathbf{q}$ to the vector $\mathbf{v}_0$ involved in defining the boundary conditions, namely in Eq. (8). To this end, examine the velocity jump at the interface $S_{\mathrm{int}} \equiv \partial V_{\mathrm{L}} \cap \partial V_{\mathrm{U}}$:

$$[\![\mathbf{v}]\!] = \mathbf{v}_0 - (\mathbf{L} + \bar{\boldsymbol{\Omega}} - \mathbf{U})\mathbf{x} \tag{B.10}$$

Continuity of the velocity across S_{int} may then be satisfied if:

$$\mathbf{v}_0 = (\mathbf{q} \otimes^{\mathrm{s}} \mathbf{n})\mathbf{x} + \bar{\boldsymbol{\Omega}}\mathbf{x} = \mathbf{q}(\mathbf{n}\cdot\mathbf{x}) + \mathbf{n}(\mathbf{q}\cdot\mathbf{x}) + \bar{\boldsymbol{\Omega}}\mathbf{x} \tag{B.11}$$

where use has been made of Eq. (B.3). Working in the $(\mathbf{m},\mathbf{n})$ axes, on S_{int} one has $\mathbf{n}\cdot\mathbf{x} = h/2$ (recall that h is the band thickness) so that:

$$\mathbf{v}_0 = \frac{h}{2}\mathbf{q} + \left(\alpha\frac{h}{2} + \beta\mathbf{m}\cdot\mathbf{x}\right)\mathbf{n} + \bar{\boldsymbol{\Omega}}\mathbf{x} \tag{B.12}$$

This equation shows that, without a judicious choice for $\bar{\boldsymbol{\Omega}}$, vector $\mathbf{v}_0$ would vary along the interface, and this would complicate matters, at least for a clean exposition. Choose:

$$\bar{\boldsymbol{\Omega}} = \bar{\Omega}_{mn}(\mathbf{m}\otimes\mathbf{n} - \mathbf{n}\otimes\mathbf{m}) \tag{B.13}$$

such that, $\forall \mathbf{x} \in S_{\mathrm{int}}$:

$$\bar{\boldsymbol{\Omega}}\mathbf{x} = \frac{h}{2}\bar{\Omega}_{mn}\mathbf{m} - (\mathbf{m}\cdot\mathbf{x})\bar{\Omega}_{mn}\mathbf{n} \tag{B.14}$$

Now, substitute this expression in Eq. (B.12) and obtain, after grouping:

$$\mathbf{v}_0 = \frac{h}{2}\mathbf{q} + \alpha\frac{h}{2}\mathbf{n} + \frac{h}{2}\bar{\Omega}_{mn}\mathbf{m} + (\beta - \bar{\Omega}_{mn})(\mathbf{m}\cdot\mathbf{x})\mathbf{n} \tag{B.15}$$

Further, specify $\bar{\boldsymbol{\Omega}}$ through:

$$\bar{\Omega}_{mn} = \beta = \frac{D_{nm}}{c} \tag{B.16}$$

This choice rids Eq. (B.15) of its last term and gives, on account of Eq. (B.9) using the shorthand notations α, β:

$$\mathbf{v}_0 = \frac{h}{2}\mathbf{q} + \frac{h}{2}(\alpha\mathbf{n} + \beta\mathbf{m}) = h\mathbf{q} \tag{B.17}$$

which is the desired result in Eq. (9) with $\mathbf{v}_0$ given by Eq. (10).

The relevant part of Eqs. (7) and (8) is on the outer boundaries (intersections of ∂V_{L} and ∂V_{U} with ∂V). One consequence of the over-constraint is that $\langle \mathbf{d} \rangle_{V_{\mathrm{L}}} = \mathbf{L}$, etc.

Appendix C. Singular parts of yield loci

Some of the yield loci depicted in Table 1 have singular parts. To determine these, the fundamental inequality underlying Eq. (15) is specialized to:

$$\forall \epsilon, \gamma, \quad \sigma\epsilon + \tau\gamma \leq \Pi(\epsilon, \gamma) \tag{C.1}$$

where σ, τ are the normal and shear tractions acting on the (homogenized) band, and ϵ, γ are, in short, the *rates* of opening and sliding. The format of Eq. (C.1) is only valid for unhomogeneous yielding; factors of two in shear terms are simply ignored since the focus is on the overall structure. Writing the above inequality for the pair $(-\epsilon, -\gamma)$ and exploiting the fact that Π is an even function, one gets:

$$\sigma\epsilon + \tau\gamma \geq -\Pi(\epsilon, \gamma) \tag{C.2}$$

Combining the two inequalities allows one to focus on $\epsilon \geq 0$ so that Eq. (C.1) is equivalent to:

$$\forall \epsilon \geq 0, \forall \gamma, \quad -\Pi(\epsilon, \gamma) \leq \sigma\epsilon + \tau\gamma \leq \Pi(\epsilon, \gamma) \tag{C.3}$$

Using the property that Π is positively homogeneous of degree 1, obtain after dividing all sides by ϵ (assuming $\epsilon \neq 0$):

$$\forall P \in \mathbb{R}, \quad -\Pi(1, P) \leq \sigma + \tau P \leq \Pi(1, P) \tag{C.4}$$

which is a form suitable for eliminating the kinematic parameter: $P = \gamma/\epsilon$.

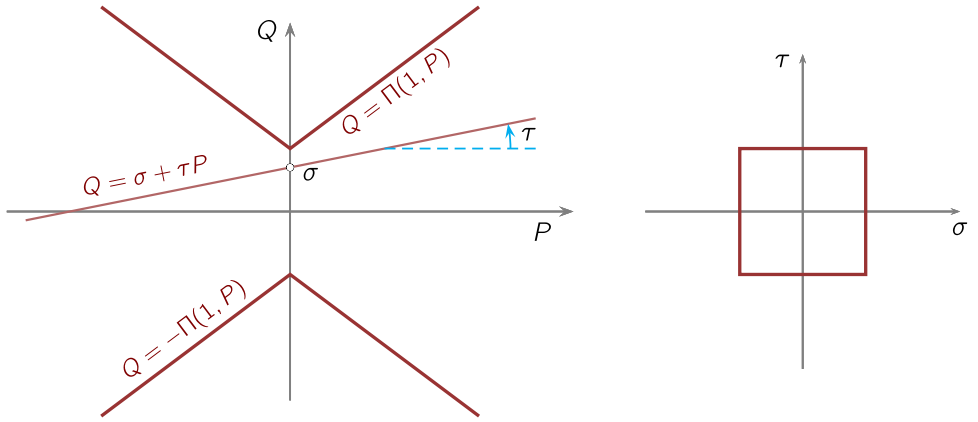

Fig. C-1. Graphical method for determining a yield locus with singular parts.

The above double inequality implies that the yield point for a given load trajectory corresponds to when the line $Q = \sigma + \tau P$ is tangent to one of the curves $Q = \Pi(1, P)$ and $Q = -\Pi(1, P)$ without crossing any of them. Owing to the symmetry of the yield locus with respect to the origin,[18] one need only determine one half of it, by considering only one of the above inequalities, namely when e.g. the line $Q = \sigma + \tau P$ meets the curve $Q = \Pi(1, P)$ without crossing it. A graphical method may be implemented to this end.

Fig. C-1 illustrates the situation for the Rankine–Tresca locus shown in the first row of Table 1. In this case, the (linear) function $Q = \Pi(1, P) = 1 + |P|$ has an angular point at $P = 0$. Begin with tensile loading as reference, the loading point $(\sigma, 0)$ belongs to the reversibility domain so long as $\sigma < 1$. When the normal stress reaches the threshold $\sigma = 1$ yielding occurs, since the horizontal line $Q = \sigma$ meets the curve $\Pi(1, P) = 1 + |P|$ at its angular point. Then with $\sigma = 1$ being maintained, upon increasing the shear stress $\tau > 0$ the loading point (σ, τ) remains on the yield locus so long as τ, which is the slope of the line $Q = \sigma + \tau P$, remains below that of the line $\Pi(1, P) = 1 + |P|$, which is unity. A similar reasoning is followed for $\tau < 0$ and the segment $(\sigma = 1, |\tau| \leq 1)$ is determined to be on the yield locus. Likewise, the segment $(\sigma = -1, |\tau| \leq 1)$ is obtained by considering the bottom curve $Q = -\Pi(1, P)$. The remaining two segments $(|\sigma| \leq 1, |\tau| = 1)$ are deduced by symmetry of the locus with respect to the pair (σ, τ) or equivalently by considering the case $\epsilon = 0$ separately in Eq. (C.3), or repeating the reasoning after Eq. (C.3) for $1/P$ and excluding the case $\gamma = 0$. *In fine*, the yield locus is a square.

A similar graphical solution was implemented by Torki et al. (2015) to obtain the criterion labeled "TBL" in Table 1.

[18] This is not valid for the "Cam-Clay" model because the corresponding dissipation function is *not* positively homogeneous, Table 1.

Appendix D. Proof of Eq. (24)

For an isotropic pore distribution, the aim is to determine the optimal band orientation for unhomogeneous yielding, i.e. find unit vector $\bar{\mathbf{n}}$ satisfying:

$$\bar{\mathbf{n}} = \underset{\mathbf{n}\in\partial\mathcal{B}}{\operatorname{argmax}}\ \phi(\sigma(\mathbf{n}),\tau(\mathbf{n})) \tag{D.1}$$

where σ and τ are given by Eq. (22). Viewing ϕ as a function of $\mathbf{n}$, the Lagrangian is written as:

$$\mathcal{L}(\mathbf{n},\lambda) = \phi^*(\mathbf{n}) - \lambda\kappa(\mathbf{n}) \tag{D.2}$$

with $\phi^*(\mathbf{n}) = \phi(\sigma(\mathbf{n}),\tau(\mathbf{n}))$, $\kappa(\mathbf{n}) = \mathbf{n}\cdot\mathbf{n} - 1$ and λ is a Lagrange multiplier. There are no critical points. Extrema of ϕ are sought among the solutions of:

$$\frac{\partial\mathcal{L}}{\partial\mathbf{n}} = \mathbf{0} \quad \text{and} \quad \mathbf{n}\cdot\mathbf{n} = 1 \tag{D.3}$$

To express the first of these obtain:

$$\frac{\partial\mathcal{L}}{\partial\mathbf{n}} = \frac{\partial\phi}{\partial\sigma}\frac{\partial\sigma}{\partial\mathbf{n}} + \frac{\partial\phi}{\partial\tau}\frac{\partial\tau}{\partial\mathbf{n}} - \lambda\frac{\partial\kappa}{\partial\mathbf{n}} \tag{D.4}$$

where, from Eq. (22),

$$\begin{cases} \dfrac{\partial\sigma}{\partial\mathbf{n}} = 2\boldsymbol{\sigma}\mathbf{n} \\ \dfrac{\partial\tau^2}{\partial\mathbf{n}} = 2(\boldsymbol{\sigma}^2 - 2\sigma\boldsymbol{\sigma})\mathbf{n} \end{cases} \tag{D.5}$$

Substituting in Eq. (D.4) gives after grouping and using Eq. $(D.3)_1$:

$$\left[\left(\frac{\partial\phi}{\partial\sigma} - \frac{\sigma}{\tau}\frac{\partial\phi}{\partial\tau}\right)\boldsymbol{\sigma} + \frac{1}{2\tau}\frac{\partial\phi}{\partial\tau}\boldsymbol{\sigma}^2\right]\mathbf{n} = \lambda\mathbf{n} \tag{D.6}$$

which is Eq. (24) on account of the definitions in Eq. (25).

Appendix E. Proof of Eq. (54)

The aim is to examine the evolution of relative pore spacing. The parameter λ^k is defined as the ratio of the mean pore spacing perpendicular to the band, $s^\perp$, to the mean spacing within the band, $\bar{s}$:

$$\lambda = \frac{s^\perp}{\bar{s}} \tag{E.1}$$

where superscript k is dropped to lighten the writing, but it is understood that all quantities in this section are relative to a single yield system k. Initial values are denoted with subscript 0. An elementary rectangular prism with dimensions $\bar{s}_0, \bar{s}_0, s_0^\perp$ represents the initial, undeformed state, Fig. E-1. After deformation, the parallelepiped has dimensions $\bar{s}, \bar{s}, s^\perp$. There is no relation between the initial and current directions by means of convective transport. However, one may relate the change in volume and area of the faces normal to the band using standard kinematical relations of continuum mechanics, namely:

$$V = \det\mathbf{F}\, V_0 \equiv J V_0 \tag{E.2}$$

with V, V_0 the current and initial volumes, and

$$\mathbf{A} = J(\mathbf{F}^{-1})^T\mathbf{A}_0 \tag{E.3}$$

where $\mathbf{A} = A\mathbf{n}$ and $\mathbf{A}_0 = A_0\mathbf{n}_0$ are the current and initial area vectors, $\mathbf{n}$ and $\mathbf{n}_0$ being the current and initial normals to the band (again dropping the index k).

Now, express Eq. (E.1) as follows:

$$\lambda = \frac{s^\perp}{s_0^\perp}\frac{s_0^\perp}{\bar{s}_0}\frac{\bar{s}_0}{\bar{s}} \tag{E.4}$$

in which the middle term is nothing but λ_0. The first term is simply:

$$\frac{s^\perp}{s_0^\perp} = \frac{V}{V_0}\frac{A_0}{A} = J\frac{A_0}{A} \tag{E.5}$$

where use was made of Eq. (E.2). From Eq. (E.3), obtain:

$$A_0\mathbf{n}_0 = \frac{A}{J}\mathbf{F}^T\mathbf{n} \quad \Rightarrow \quad A_0 = \frac{A}{J}\|\mathbf{F}^T\mathbf{n}\| \tag{E.6}$$

Combining Eqs. (E.5) and (E.6) gives:

$$\frac{s^\perp}{s_0^\perp} = \|\mathbf{F}^T\mathbf{n}\| \tag{E.7}$$

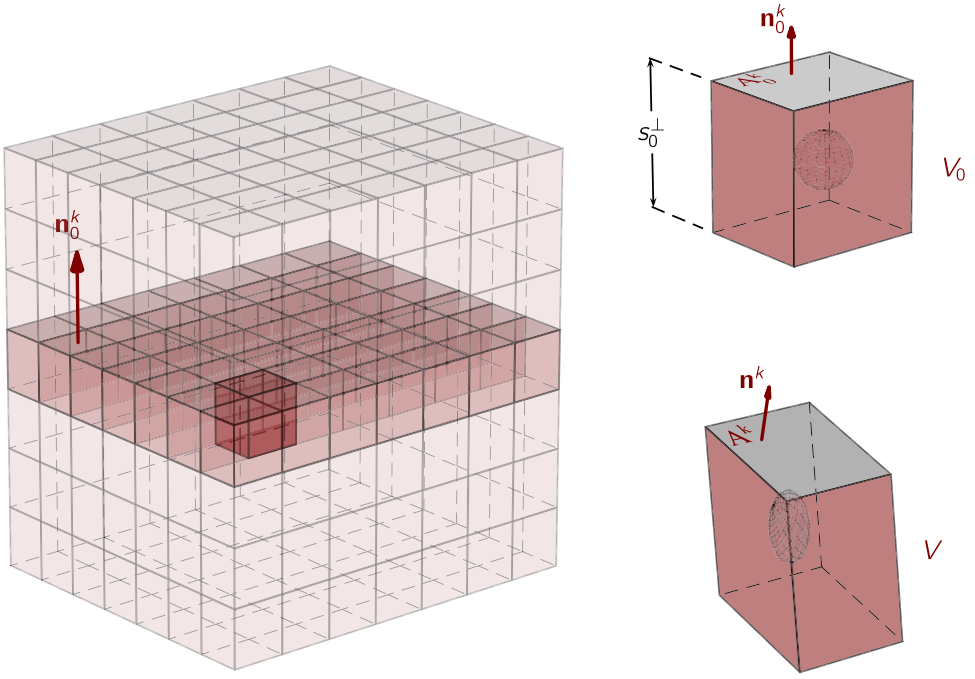

Fig. E-1. Elementary cell within a band of unhomogeneous yielding.

Finally, the last term in Eq. (E.4) is approximated by:

$$\frac{\bar{s}_0}{\bar{s}} = \sqrt{\frac{A_0}{A}} \tag{E.8}$$

The above holds exactly for a periodic void distribution and is a reasonable approximation for an *ordered* arrangement of pores (weak variance about the means).

Using again Eq. $(E.6)_2$ to estimate the right-hand side of Eq. (E.8) and substituting back in Eq. (E.4) leads to:

$$\lambda = \frac{\lambda_0}{\sqrt{J}} \|\mathbf{F}^T\mathbf{n}\|^{\frac{3}{2}} \tag{E.9}$$

in which the euclidean norm is nothing but:

$$\|\mathbf{F}^T\mathbf{n}\| = \sqrt{\mathbf{F}^T\mathbf{n}\cdot\mathbf{F}^T\mathbf{n}} = \sqrt{\mathbf{n}\cdot\mathbf{F}(\mathbf{F}^T\mathbf{n})} = \sqrt{\mathbf{n}\cdot(\mathbf{F}\mathbf{F}^T)\mathbf{n}} \tag{E.10}$$

so that Eq. (54) is obtained.

Appendix F. Evolution of the pore axes

The aim is to elicit, for unhomogeneous yielding, the general structure of the average strain-rate and rotation-rate of the pores, $\mathbf{D}^{\mathrm{v}}$ and $\boldsymbol{\Omega}^{\mathrm{v}}$, entering Eq. (56) and, correspondingly, the structure of concentration tensors $\mathbb{C}^k$ and $\mathbb{R}^k$ entering Eq. (57). For simplicity, the index k will be dropped.

Using homogenization, Ponte Castañeda and Zaidman (1994) derived the following relation between $\mathbf{D}^{\mathrm{v}}$ and the overall rate of deformation $\mathbf{D}$ for an ellipsoidal void embedded in an isotropic incompressible *elastic* medium:

$$\mathbf{D}^{\mathrm{v}} = [\mathbb{I} - (1-f)\mathbb{S}]^{-1} : \mathbf{D} \equiv \mathbb{C}^{\mathrm{el}} : \mathbf{D} \tag{F.1}$$

where $\mathbb{S}$ denotes Eshelby's (1957) first tensor and $\mathbb{I}$ the fourth-order identity tensor. Later, Kailasam and Ponte Castaneda (1998) developed a relation between $\boldsymbol{\Omega}^{\mathrm{v}}$ and $\mathbf{D}$, under the same conditions,

$$\boldsymbol{\Omega}^{\mathrm{v}} = \boldsymbol{\Omega} + (1-f)\mathbb{P} : (\mathbb{C}^{\mathrm{el}} : \mathbf{D}) \equiv \boldsymbol{\Omega} + \mathbb{R}^{\mathrm{el}} : \mathbf{D} \tag{F.2}$$

where $\mathbb{P}$ denotes Eshelby's (1957) second tensor. Tensor $\mathbb{C}^{\rm el}$ possesses minor (but no major) symmetries, while $\mathbb{R}^{\rm el}$ is antisymmetric in its first two indices and symmetric in its last two. Madou et al. (2013) adopted the above two formats, replacing the elastic concentration tensors, $\mathbb{C}^{\rm el}$ and $\mathbb{R}^{\rm el}$, with plastic ones that included heuristic corrections guided by numerical limit analysis results. Their derivations, however, are applicable to homogeneous yielding only.

For unhomogeneous yielding, one possible approach would be to adopt the Madou–Leblond equations within the band thereby replacing the plastic strain-rate with $\mathbf{D}^{\rm p}/c$ where c is the band volume fraction. Another approach would be to adopt the format but recalculate the plastic correction factors based on appropriate numerical limit analysis calculations. The latter would have merits but assumes an elastic format basis as appropriate for unhomogeneous yielding. That is not so obvious on account of the highly constrained plastic flow during that regime.

The most natural, and incidentally simpler and more accurate, approach consists of using essential traits of unhomogeneous deformation, as embodied in the boundary conditions of Eqs. (7) and (8) augmented with Benzerga's (2002) conjecture, namely that the band thickness is about the void dimension perpendicular to the band. The first element leads to recognizing that the only relevant components of the overall strain-rate are: $\dot{\epsilon} \equiv D_{nn}$ (extension normal to the band) and $\dot{\gamma} \equiv D_{nm}$ (shearing parallel to the band). By way of consequence, $\mathbf{D}^{\rm v}$ only has three relevant components assuming transverse isotropy with respect to the band. Therefore, there are (at most) six independent concentration factors entering $\mathbb{C}$. Likewise, $\boldsymbol{\Omega}^{\rm v}$ only has one relevant component. Mathematically, one may write in reduced form:

$$\bar{\mathbf{D}}^{\rm v} = \bar{\mathbf{C}}\bar{\mathbf{D}}^{\rm p} \tag{F.3}$$

where:

$$\bar{\mathbf{D}}^{\rm v} = \begin{Bmatrix} D^{\rm v}_{mm} \\ D^{\rm v}_{nn} \\ D^{\rm v}_{mn} \end{Bmatrix} \qquad \bar{\mathbf{D}}^{\rm p} = \begin{Bmatrix} \dot{\epsilon} \\ \dot{\gamma} \end{Bmatrix} \qquad \bar{\mathbf{C}} = \begin{pmatrix} C_{11} & C_{12} \\ C_{21} & C_{22} \\ C_{31} & C_{32} \end{pmatrix} \tag{F.4}$$

That matrix $\bar{\mathbf{C}}$ is not square reflects that even if the band were to undergo a pure extension, the void would expand laterally, an essential trait of void coalescence for instance.

Likewise,

$$\Omega^{\rm v}_{mn} = \Omega_{mn} + \bar{R}_1\dot{\epsilon} + \bar{R}_2\dot{\gamma} \tag{F.5}$$

where, on account of the relation $\Omega^{\rm v}_{mn} = \Omega_{mn} + (1-f)P_{mnmn}D^{\rm v}_{mn}$ (no sum) the two coefficients are:

$$\bar{R}_1 = (1-f)P_{mnmn}C_{31}, \qquad \bar{R}_2 = (1-f)P_{mnmn}C_{32} \tag{F.6}$$

The specific dependence of the C_{ij} coefficients vis-a-vis geometrical descriptors, including but not limited to f and c, as well as a single component of $\mathbb{P}$, may be obtained by combining Benzerga's (2002) conjecture with plastic incompressibility of the matrix material. For example, in the absence of shear, the equations of Benzerga (2002) may be recast in the format of Eq. (F.4) with:

$$C_{11} = \frac{1}{2}\left[\frac{1}{f} - \frac{1}{c}\right], \qquad C_{21} = \frac{1}{c}, \qquad C_{ij} = 0 \text{ otherwise} \tag{F.7}$$

General expressions for the C_{ij} coefficients remain to be developed for general loadings. Whatever they may be, the evolution of the pore axes has the general structure embodied by Eqs. (F.3) to (F.6) along with Eq. (57).

Appendix G. Yielding mode with hardening

For clarity, we introduce the function $\sigma = \sigma^{\rm uni}(\epsilon)$ to represent an isotropic hardening law relating the logarithmic (Hencky) strain to the true stress in a uniaxial loading experiment.

G.1. High triaxiality

Proposition. *A porous material with a strain-hardenable matrix yields homogeneously at sufficiently high triaxiality and sufficiently low porosity.*

Before elaborating on this, a word on significance is needed. Indeed, in a non-hardening matrix, the opposite would be expected, even though this itself is contrary to current common belief. To be clear, a porous material with a non-hardening matrix would yield *unhomogeneously* at sufficiently high triaxiality, at least in the $f > 0.01$ porosity regime. To see this, simply note that the exact homogeneous-yield pressure is very close to the only estimate we know of for the unhomogeneous-yield pressure (see Section 5.4 and Fig. 4). But the latter is a rigorous upper bound whereas the former is an exact solution.[19] It follows that the exact unhomogeneous-yield pressure (which is not known) must be below the homogeneous-yield pressure. This argument holds regardless of the assumed shape of the yield surface, see Section 5.4.

[19] The upper bound is for equiaxed cylindrical cavities oriented at random. The exact solution is for the hollow sphere. The argument lacks therefore complete certainty.

Rationale. We make two assumptions:

$\mathcal{A}_1$: *Strain concentration under unhomogeneous yielding is more intense than under homogeneous yielding.*

$\mathcal{A}_2$: *A heuristic extension to hardening of any porous plasticity criterion amounts to evaluating the flow stress for the plastic strain averaged over the plastic zone. By way of contrast, the exact solution involves a weighted average of the flow stress itself over the plastic zone.*

Assumption $\mathcal{A}_1$ is reasonable given the high constraint imposed by the presence of elastically unloaded zones above and the below the pore in the UY mode. It is supported by available direct numerical simulations of voided cells.

Assumption $\mathcal{A}_2$ is true for purely hydrostatic loading. Indeed, the homogeneous-yield pressure emerging from Eqs. (67) and (70) or Eqs. (67) and (71) is $\sigma_{\rm m}^{\rm Gur} = a\bar{\sigma} = a(f)\sigma^{\rm uni}(\epsilon^*)$. Perrin (1992) has shown that this estimate, applied to a hollow sphere, can be written as:

$$\sigma_{\rm m}^{\rm Gur} = a\sigma^{\rm uni}\left(\frac{\int_r^R \bar{\epsilon}\,\rho^2\,{\rm d}\rho}{\int_r^R \rho^2\,{\rm d}\rho}\right) = a\sigma^{\rm uni}\left(\langle\bar{\epsilon}(\mathbf{x})\rangle_{V^{\rm m}}\right) \tag{G.1}$$

with r and R denoting the inner and outer radii of the sphere. On the other hand, the exact homogeneous-yield pressure for a hollow sphere made of a hardenable matrix is known to be (ρ_0 denoting the current radius before straining):

$$\sigma_{\rm m}^{\rm H} = 2\int_r^R \sigma^{\rm uni}\left(2\ln\frac{\rho}{\rho_0}\right)\frac{{\rm d}\rho}{\rho} \tag{G.2}$$

which can be put in the form:

$$\sigma_{\rm m}^{\rm H} = a\left(\frac{\int_r^R \sigma^{\rm uni}(\bar{\epsilon})\,\frac{{\rm d}\rho}{\rho}}{\int_r^R \frac{{\rm d}\rho}{\rho}}\right) = a\langle\!\langle\sigma^{\rm uni}(\bar{\epsilon}(\mathbf{x}))\rangle\!\rangle_{V^{\rm m}} \tag{G.3}$$

Therefore, while the heuristic estimate of Eq. (G.1) amounts to taking the actual volume average of $\bar{\epsilon}$ over the matrix volume $V^{\rm m}$, the exact value in Eq. (G.3) involves a weighted average of the flow stress itself.

By virtue of $\mathcal{A}_2$, now applied to unhomogeneous yielding, one may write:

$$\sigma_{\rm m}^{\rm U,heur} = a\sigma^{\rm uni}\left(\langle\bar{\epsilon}(\mathbf{x})\rangle_{V_{\rm L}}\right) \tag{G.4}$$

and

$$\sigma_{\rm m}^{\rm U} = a\langle\!\langle\sigma^{\rm uni}(\bar{\epsilon}(\mathbf{x}))\rangle\!\rangle_{V_{\rm L}} \tag{G.5}$$

Two inequalities hold unconditionally:

$$\sigma_{\rm m}^{\rm Gur} < \sigma_{\rm m}^{\rm H} \tag{G.6}$$

$$\sigma_{\rm m}^{\rm U,heur} < \sigma_{\rm m}^{\rm U} \tag{G.7}$$

The following ones hold conditionally:

$$\sigma_{\rm m}^{\rm U,heur} \lesssim \sigma_{\rm m}^{\rm Gur} \tag{G.8}$$

$$\sigma_{\rm m}^{\rm U} > \sigma_{\rm m}^{\rm H} \tag{G.9}$$

Inequality (G.6) was established by Perrin (1992). The proof of (G.7) follows along the same lines with some difficulties that are not worth elaborating upon as both inequalities are tangential to the proposition.

The statement in (G.8) follows from the discussion in Section 5.4. But the point of the proposition is embodied in inequality (G.9). The key resides in the fact that exact yield stresses $\sigma_{\rm m}^{\rm H}$ and $\sigma_{\rm m}^{\rm U}$ in Eqs. (G.3) and (G.5) involve the weighted average. The actual average involves integration measure $\rho^2\,{\rm d}\rho$. By way of contrast, the weighted average involves a different measure, ${\rm d}\rho/\rho$, which favors regions in the vicinity of the void over regions away from it. This, combined with a stronger gradient of the flow stress, by virtue of assumption $\mathcal{A}_1$, delivers the desired result. The reason this argument does not hold when comparing the heuristic estimates is that the spatial average gives more weight to regions away from the void so that local gradients (near the void) become inconsequential.

That inequality (G.9) is conditionally true results from the porosity dependence of the two modes of yielding not being the same. In an evolution problem, this is reflected in a competition between strain-hardening and porosity-softening. The porosity-dependence of the inequality manifests in a critical value of some effective strain above which unhomogeneous yielding is bound to become dominant again, as it is for the nonhardening case or with the heuristic extensions.

Once (G.9) is established, the proposition follows immediately from the shapes of the yield surfaces near the hydrostatic axes with the UY surface exhibiting a corner and the HY one being smooth.

G.2. Low triaxiality

There is a remarkable duality in the reasoning for the extreme cases of pure pressure or pure shear loading. Admit approximations $\mathcal{A}_1$ and $\mathcal{A}_2$. Then the above proposition holds true for shear loading. The counterparts of inequalities (G.6) and (G.7) remain valid with $\sigma_{\rm m}$ replaced everywhere with the yield stress in shear. The counterpart to (G.8) is now a *rigorous* and strict inequality (see Eq. (79) in the main text). The counterpart of (G.9), which is Eq. (80) then follows.

Appendix H. Proof of Eq. (111)

The result, which was established by Gologanu et al. (1997), is reproduced here for ease of accessibility. Start from the indicial form of Eq. (110):

$$v_i = A_{ij}x_j + B_{ijk}x_jx_k \tag{H.1}$$

By definition of the volume average, Eq. (1), obtain:

$$\langle d_{ij}\rangle = \frac{1}{2V}\int_{\partial V}\left[A_{ik}x_kn_j + \frac{1}{2}B_{ikm}x_kx_mn_j + A_{jk}x_kn_i + \frac{1}{2}B_{jkm}x_kx_mn_i\right]\mathrm{d}S \tag{H.2}$$

where the boundary condition, Eq. (H.1) has been used. Applying the divergence theorem,

$$\begin{aligned}\langle d_{ij}\rangle &= \frac{1}{2V}\int_{V}\left[A_{ik}\delta_{kj} + \frac{1}{2}B_{ikm}(\delta_{kj}x_m + x_k\delta_{mj}) + A_{jk}\delta_{ki} + \frac{1}{2}B_{jkm}(\delta_{ki}x_m + x_k\delta_{mi})\right]\mathrm{d}V\\ &= \frac{1}{2V}\int_{V}\left[A_{ij} + A_{ji} + \frac{1}{2}(B_{ijm}x_m + B_{ikj}x_k + B_{jim}x_m + B_{jki}x_k)\right]\mathrm{d}V\end{aligned} \tag{H.3}$$

Using the symmetry of $\mathbf{A}$ and the symmetry of $\mathbf{B}$ in the last two indices ($B_{ikj} = B_{ijk}$ and $B_{jki} = B_{jik}$), obtain after grouping like terms (k and m being dummy):

$$\langle d_{ij}\rangle = \frac{1}{2V}\int_{V}2A_{ij} + (B_{ijk} + B_{jik})x_k\,\mathrm{d}V \tag{H.4}$$

which delivers Eq. (111), $\mathbf{A}$ and $\mathbf{B}$ being constant and account being taken of the definition in Eq. (112).

Appendix I. Convexity of the reversibility domain

Given the linearity of the mapping between thermodynamic forces and the pair $(\boldsymbol{\sigma}, \bar{\sigma})$, what needs to be shown is that the set (keeping the notation $\bar{C}$):

$$\bar{C} \equiv \{(\boldsymbol{\sigma}, \bar{\sigma})\,|\quad \boldsymbol{\Phi}^{\mathrm{U}}(\boldsymbol{\sigma}, \bar{\sigma}, f_b) \le 0\} \tag{I.1}$$

is convex. This is not obvious because $\boldsymbol{\Phi}^{\mathrm{U}}(\boldsymbol{\sigma}, \bar{\sigma}, f_b)$ is not convex with respect to the pair $(\boldsymbol{\sigma}, \bar{\sigma})$ for any of the yield criteria considered, say in Table 1.

Define now a new set as:

$$\hat{C} \equiv \{\hat{\boldsymbol{\sigma}}\,|\quad \hat{\boldsymbol{\Phi}}^{\mathrm{U}}(\hat{\boldsymbol{\sigma}}; f_b) \le 0\} \tag{I.2}$$

where $\hat{\boldsymbol{\Phi}}^{\mathrm{U}}(\hat{\boldsymbol{\sigma}}; f_b) = \boldsymbol{\Phi}^{\mathrm{U}}(\boldsymbol{\sigma}, \bar{\sigma}, f_b)$ and $\hat{\boldsymbol{\sigma}} \equiv \boldsymbol{\sigma}/\bar{\sigma}$. Because $\boldsymbol{\Phi}^{\mathrm{U}}$ is convex with respect to $\boldsymbol{\sigma}$,[20] $\hat{\boldsymbol{\Phi}}^{\mathrm{U}}$ is convex with respect to $\hat{\boldsymbol{\sigma}}$ so that $\hat{C}$ is convex. Clearly,

$$(\boldsymbol{\sigma}, \bar{\sigma}) \in \bar{C} \Leftrightarrow \hat{\boldsymbol{\sigma}} \in \hat{C} \tag{I.3}$$

Given two pairs $(\boldsymbol{\sigma}_1, \bar{\sigma}_1)$ and $(\boldsymbol{\sigma}_2, \bar{\sigma}_2)$ in $\bar{C}$, one needs to show that:

$$\forall\zeta \in [0,1],\quad \Big((1-\zeta)\boldsymbol{\sigma}_1 + \zeta\boldsymbol{\sigma}_2, (1-\zeta)\bar{\sigma}_1 + \zeta\bar{\sigma}_2\Big) \in \bar{C} \tag{I.4}$$

or equivalently, given Eq. (I.3), that

$$\forall\zeta \in [0,1],\quad \hat{\boldsymbol{\Sigma}} \equiv \frac{(1-\zeta)\boldsymbol{\sigma}_1 + \zeta\boldsymbol{\sigma}_2}{(1-\zeta)\bar{\sigma}_1 + \zeta\bar{\sigma}_2} \in \hat{C} \tag{I.5}$$

Let $\hat{\boldsymbol{\sigma}}_1 \equiv \boldsymbol{\sigma}_1/\bar{\sigma}_1$ and $\hat{\boldsymbol{\sigma}}_2 \equiv \boldsymbol{\sigma}_2/\bar{\sigma}_2$ then both are in $\hat{C}$ and one may write:

$$\hat{\boldsymbol{\Sigma}} = \frac{(1-\zeta)\bar{\sigma}_1}{(1-\zeta)\bar{\sigma}_1 + \zeta\bar{\sigma}_2}\hat{\boldsymbol{\sigma}}_1 + \frac{\zeta\bar{\sigma}_2}{(1-\zeta)\bar{\sigma}_1 + \zeta\bar{\sigma}_2}\hat{\boldsymbol{\sigma}}_2 \tag{I.6}$$

which is of the form $(1-\zeta')\hat{\boldsymbol{\sigma}}_1 + \zeta'\hat{\boldsymbol{\sigma}}_2$ with $\zeta' \in [0,1]$. Therefore, $\hat{\boldsymbol{\Sigma}} \in \hat{C}$ and Eq. (I.5) is satisfied. Hence, Eq. (I.4) is proven and $\bar{C}$ is convex.

References

Anand, L., Kothari, M., 1996. A computational procedure for rate-independent crystal plasticity. J. Mech. Phys. Solids 44, 525–558.
Benallal, A., Desmorat, R., Fournage, M., 2014. An assessment of the role of the third stress invariant in the Gurson approach for ductile fracture. Eur. J. Mech. A Solids 47, 400–414.
Benzerga, A.A., 2002. Micromechanics of coalescence in ductile fracture. J. Mech. Phys. Solids 50, 1331–1362.
Benzerga, A.A., Bréchet, Y., Needleman, A., Van der Giessen, E., 2005. The stored energy of cold work: predictions from discrete dislocation plasticity. Acta Mater. 53, 4765–4779.

[20] This is by definition in Section 9 and as a property resulting from the general structure in Section 4.2.

Benzerga, A.A., Leblond, J.B., 2010. Ductile fracture by void growth to coalescence. Adv. Appl. Mech. 44, 169–305.
Benzerga, A.A., Leblond, J.B., 2014. Effective yield criterion accounting for microvoid coalescence. J. Appl. Mech. 81, 031009.
Benzerga, A.A., Leblond, J.B., Needleman, A., Tvergaard, V., 2016. Ductile failure modeling. Int. J. Frac. 201, 29–80.
Besson, J., 2009. Damage of ductile materials deforming under multiple plastic or viscoplastic mechanisms. Int. J. Plast. 25, 2204–2221.
Cazacu, O., Revil-Baudard, B., Chandola, N., Kondo, D., 2014. New analytical criterion for porous solids with Tresca matrix under axisymmetric loadings. Int. J. Solids Struct. 51, 861–874.
Drucker, D.C., 1966. Continuum theory of plasticity on macroscale and microscale. J. Mater. 1 (873).
Drucker, D.C., Prager, W., Greenberg, M.J., 1952. Extended limit analysis theorems for continuous media. Q. Appl. Math. 9, 381–389.
Enakoutsa, K., Leblond, J.B., Perrin, G., 2007. Numerical implementation and assessment of a phenomenological nonlocal model of ductile rupture. Comput. Methods Appl. Mech. Engrg. 196, 1946–1957.
Eshelby, J.D., 1957. The determination of the elastic field of an ellipsoidal inclusion, and related problems. Proc. R. Soc. Lond. Ser. A 241, 376–396.
Gologanu, M., Leblond, J.B., Perrin, G., Devaux, J., 1997. Recent extensions of Gurson's model for porous ductile metals. In: Suquet, P. (Ed.), Continuum Micromechanics. In: CISM Lectures Series, Springer, New York, pp. 61–130.
Green, R.J., 1972. A plasticity theory for porous solids. Int. J. Mech. Sci. 14, 215–224.
Gurson, A.L., 1977. Continuum theory of ductile rupture by void nucleation and growth: Part I– yield criteria and flow rules for porous ductile media. J. Eng. Mater. Technol. 99, 2–15.
Halphen, B., Son, N.Q., 1975. Sur les matériaux standards généralisés. J. de Mécanique 14, 39–63.
Hill, R., 1950. the Mathematical Theory of Plasticity. Clarendon Press, Oxford.
Hill, R., 1951. On the state of stress in a plastic-rigid body at the yield point. Philos. Mag. 42, 868–875.
Hill, R., 1967. The essential structure of constitutive laws for metal composites and polycrystals. J. Mech. Phys. Solids 15, 79–95.
Huang, Y., Hutchinson, J.W., Tvergaard, V., 1991. Cavitation instabilities in elastic–plastic solids. J. Mech. Phys. Solids 39, 223–241.
Kailasam, M., Ponte Castaneda, P., 1998. A general constitutive theory for linear and nonlinear particulate media with microstructure evolution. J. Mech. Phys. Solids 46, 427–465.
Keralavarma, S.M., 2017. A multi-surface plasticity model for ductile fracture simulations. J. Mech. Phys. Solids 103, 100–120.
Keralavarma, S.M., Chockalingam, S., 2016. A criterion for void coalescence in anisotropic ductile materials. Int. J. Plast. 82, 159–176.
Koplik, J., Needleman, A., 1988. Void growth and coalescence in porous plastic solids. Int. J. Solids Struct. 24, 835–853.
Labuz, J.F., Zang, A., 2012. Mohr–Coulomb failure criterion. Rock Mech. Rock Eng. 45, 975–979.
Leblond, J.B., Kondo, D., Morin, L., Remmal, A., 2018. Classical and sequential limit analysis revisited. C. R. Mecanique 346, 336–349.
Leblond, J.B., Morin, L., 2014. Gurson's criterion and its derivation revisited. J. Appl. Mech. 81, 051012.
Leblond, J.B., Mottet, G., 2008. A theoretical approach of strain localization within thin planar bands in porous ductile materials. C. R. Mecanique 336, 176–189.
Leblond, J.B., Perrin, G., Devaux, J., 1995. An improved Gurson–type model for hardenable ductile metals. Eur. J. Mechs, A/Solids 14, 499–527.
Leblond, J.B., Perrin, G., Suquet, P., 1994. Exact results and approximate models for porous viscoplastic solids. Int. J. Plast. 10, 213–225.
Madou, K., Leblond, J.B., 2012. A Gurson-type criterion for porous ductile solids containing arbitrary ellipsoidal voids – I: Limit-analysis of some representative cell. J. Mech. Phys. Solids 60, 1020–1036.
Madou, K., Leblond, J.B., Morin, L., 2013. Numerical studies of porous ductile materials containing arbitrary ellipsoidal voids —II: Evolution of the length and orientation of the void axes. Eur. J. Mech. A Solids 42, 490–507.
Mandel, J., 1964. Contribution théorique à l'étude de l'écrouissage et des lois d'écoulement plastique. In: 11^{Th} International Congress on Applied Mechanics. Springer, Berlin, pp. 502–509.
McClintock, F.A., 1968. A criterion for ductile fracture by the growth of holes. J. Appl. Mech. 35, 363–371.
Michel, J.C., Suquet, P., 1992. The constitutive law of nonlinear viscous and porous materials. J. Mech. Phys. Solids 40, 783–812.
Morin, L., Leblond, J., Benzerga, A.A., Kondo, D., 2016. A unified criterion for the growth and coalescence of microvoids. J. Mech. Phys. Solids 97, 19–36.
Morin, L., Michel, J.C., Leblond, J.B., 2017. A Gurson-type layer model for ductile porous solids with isotropic and kinematic hardening. Int. J. Solids Struct. 118, 167–178.
Nemat-Nasser, S., Hori, M., 1993. Micromechanics: Overall Properties of Heterogeneous Materials. Elsevier, Amsterdam.
Pan, J., Saje, M., Needleman, A., 1983. Localization of deformation in rate sensitive porous plastic solids. Int. J. Frac. 21, 261–278.
Perrin, G., 1992. Contribution à l'étude théorique et numérique de la rupture ductile des métaux. (Ph.D. thesis). Ecole Polytechnique.
Ponte Castaneda, P., Suquet, P., 1997. Nonlinear composites. Adv. Appl. Mech. 34, 171–302.
Ponte Castañeda, P., Willis, J.R., 1995. The effect of spatial distribution on the effective behavior of composite materials and cracked media. J. Mech. Phys. Solids 43, 1919–1951.
Ponte Castañeda, P., Zaidman, M., 1994. Constitutive models for porous materials with evolving microstructure. J. Mech. Phys. Solids 42, 1459–1495.
Rice, J.R., 1976. The localization of plastic deformation. In: Koiter, W.T. (Ed.), 14th Int. Cong. Theoretical and Applied Mechanics. North–Holland Publishing Co, Amsterdam, pp. 207–220.
Rousselier, G., 1987. Ductile fracture models and their potential in local approach of fracture. Nucl. Eng. Des. 105, 97–111.
Tekoglu, C., Leblond, J.B., Pardoen, T., 2012. A criterion for the onset of void coalescence under combined tension and shear. J. Mech. Phys. Solids 60, 1363–1381.
Torki, M.E., Benzerga, A.A., Leblond, J.B., 2015. On void coalescence under combined tension and shear. J. Appl. Mech. 82, 071005.
Torki, M.T., Keralavarma, S.M., Benzerga, A.A., 2021. An analysis of Lode effects in ductile failure. J. Mech. Phys. Solids 153, 104468.
Tvergaard, V., 1982. On localization in ductile materials containing spherical voids. Int. J. Frac. 18, 237–252.
Willis, J.R., 1977. Bounds and self-consistent estimates for the overall properties of anisotropic composites. J. Mech. Phys. Solids 25, 185–202.